FUNCTIONAL AND CATEGORICAL ANALYSIS OF WAVESHAPES RECORDED ON MICROELECTRODE ARRAYS

Jacob C. Schwartz, B.S.

Thesis Prepared for the Degree of

MASTER OF SCIENCE

UNIVERSITY OF NORTH TEXAS

May 2005

APPROVED:

Guenter W. Gross, Major Professor
Jannon Fuchs, Committee Member
Harris Schwark, Committee Member
Art Goven, Chair of Department of Biological Sciences
Sandra L. Terrell, Dean of the Robert B. Toulouse School of Graduate Studies

Schwartz, Jacob C., Functional and Categorical Analysis of Waveshapes Recorded on Microelectrode Arrays. Master of Science (Biology), May 2005, 66 pp., 7 tables, 19 illustrations, references, 37 titles.

Dissociated neuronal cell cultures grown on substrate integrated microelectrode arrays (MEAs) generate spontaneous activity that can be recorded for up to several weeks. The signature wave shapes from extracellular recording of neuronal activity display a great variety of shapes with triphasic signals predominating. I characterized extracellular recordings from over 600 neuronal signals. I have preformed a categorical study by dividing wave shapes into two major classes: (type 1) signals in which the large positive peak follows the negative spike, and (type 2) signals in which the large positive peak precedes the negative spike. The former are hypothesized to be active signal propagation that can occur in the axon and possibly in soma or dendrites. The latter are hypothesized to be passive which is generally secluded to soma or dendrites. In order to verify these hypotheses, I pharmacologically targeted ion channels with tetrodotoxin (TTX), tetraethylammonium (TEA), 4-aminopyridine (4-AP), and monensin.

TABLE OF CONTENTS

Page

LIST OF TABLES

Page

LIST OF FIGURES

Page

CHAPTER 1

INTRODUCTION

1.1 Objective, Specific Aims, and Significance

The goal of this thesis is to establish a protocol and method for investigations into ion channel pharmacology and functional significance using multi electrode arrays and to conduct preliminary investigations using ion channel blockers, temperature, and age as variables. The objective is to characterize the types and prevalence of action potential (AP) shapes recorded from cultured neuronal networks growing on substrate-integrated microelectrode arrays. In addition, comparisons to *in vivo* studies and attempts to extrapolate from extracellular to intracellular patch clamp studies were made. The specific aims are as follows.

1) Validate waveshape analysis study using response of AP shapes to temperature at 27, 32, and 37 °C.
2) Measure the response of AP shapes to potassium channel and sodium channel modulators.
3) Measure the development of AP shapes from weeks 3 through 7 *in vitro* and categorize AP shape types.

The significance of understanding the action potential shapes is that it would allow researchers using microelectrode arrays to identify neurons by their sensitivity to ion channel blockers, study the functional significance of ion channels, study membrane plasticity, study the pharmacology of cell compartments separately, and to conduct long term studies on ion channels.

CHAPTER 2

BACKGROUND

2.1 Ion Channels

The expression of ion channels by neurons has an interesting evolution during development and may be implicated in the cause or treatment of a number of neurological disorders, such as epilepsy [Gao and Ziskand, 1998; Traub et al., 1999; Kaneko et al., 2002], multiple sclerosis [Bostock et al., 1981; Sheratt et al., 1980; Reganathan et al., 2003], and spinal cord injury [Nashmi and Fehling, 2001]. In addition, Na^+ and K^+ channel types and densities differ between different neuronal compartments and among various neuron types. These differences are most likely major contributing factors for the intrinsic firing properties of neurons [Nashmi and Fehling, 2001; Stuart and Sakmann, 1994; Waxman et al., 2000]. The complexity of this field is baffling. However, as mentioned above, there exists the strong potential for discovery of novel therapeutic targets [Waxman et al., 2000].

Electrophysiology can reveal the functional importance of the ion channel in determining network dynamics [Gao and Ziskand, 1998]. Hitherto, ion channel electrophysiology has focused on patch clamping of single cells. Due to technical difficulty *in vivo* associated with both accessing deeper tissues and drug applications, these methods often require either slice preparations [Gao and Ziskand, 1998] or dissection of neurons from network [Safronov, 1999]. In both cases, ion channels are not behaving in the native, spontaneously active state and only one neuron can be researched at a time.

New improvements in the theory of ion channel involvement in conductance and the current relationship to extracellular AP shapes, have made it feasible to study population ion

channel currents extracellularly. More importantly, it is possible to determine the functional importance of specific sub-types of ion channels for network dynamics using pharmacology or even gene transfection. In addition, improvements in recording equipment, software, and data analysis software have also made it possible to measure minute AP shape fluctuations due to ion current modulations.

2.2 Action Potentials

It is well known that action potentials are the result of a negative, inward sodium current followed by a positive, outward potassium current [Hodgkin and Huxley, 1952]. Several different types of signals are produced by neurons and can be observed extracellularly [Llinas and Nicholson, 1971; Henze et al., 2000; Holt, 1998; Buzsaki & Kandel, 1998] (Figure 2). Many extracellular recordings of action potentials strongly resemble the membrane current measurements or a delayed derivative of the potential signal with a strong negative peak, sometimes preceded by slight positive peak, and followed by a long positive peak. Freygang and Frank [1959] have demonstrated that the extracellular signal of an actively propagated action potential recorded by an electrode near the axon is directly proportional to the membrane current by a factor of the time constant for the membrane (Figure 3).

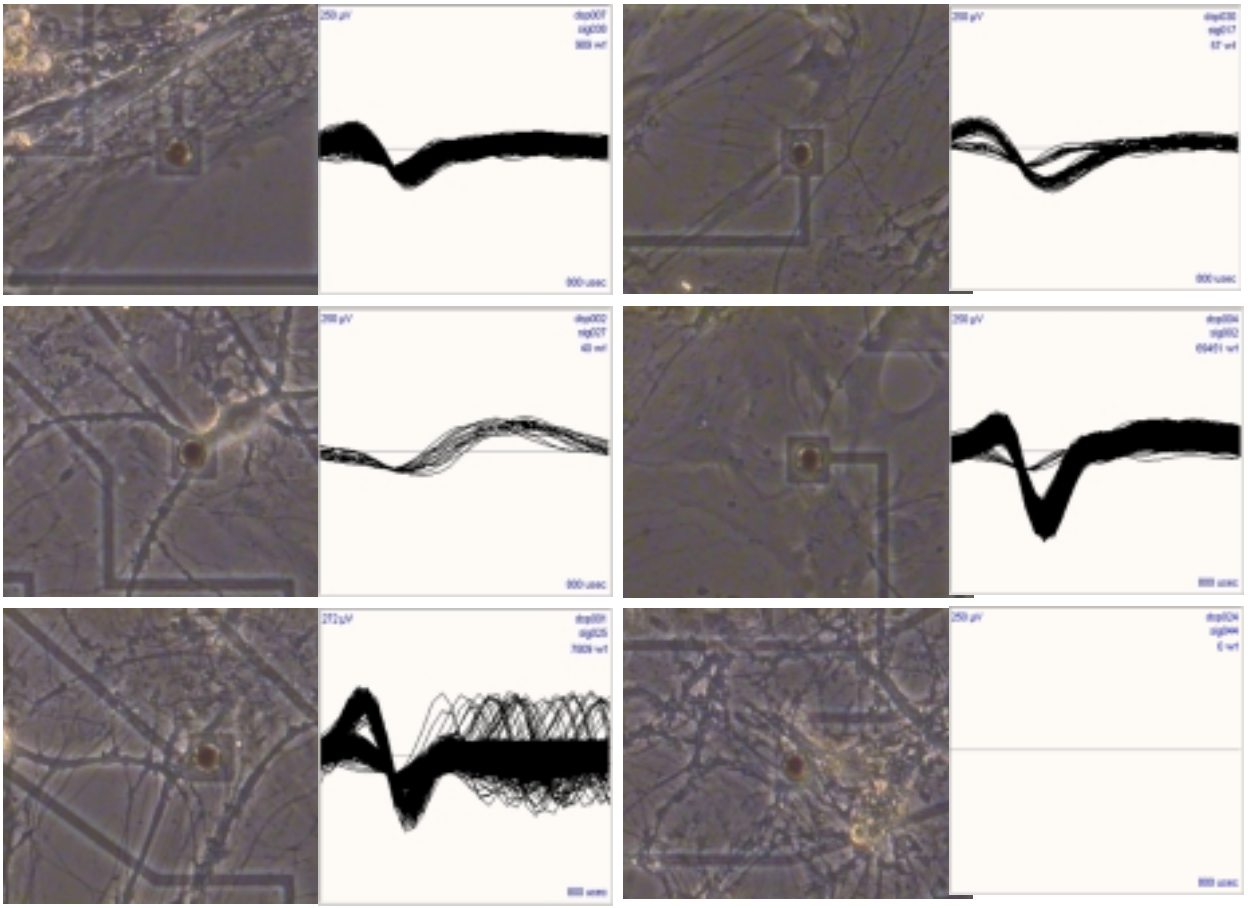

Figure 1: WAVESHAPE RECORDED AT EACH ELECTRODE. For each image of the electrode environment, the corresponding recording on the right reveals that visual inspection might not be predictive since surrounding glial cells may obscure a process or shield the electrode from electrical signaling. In the lower left panel, no signals are observed despite a thick tangle of processes near the electrode.

However, there are other types of shapes recorded extracellularly that do not resemble the membrane current plots. These signals have a large positive peak, followed by a large negative peak and a small positive peak. Rall and Humphrey have established a theory of passive

conductance, which explains that these other types of shapes are the result of passive conductance such as might occur in the soma or dendrites [Rall, 1962; Humphrey, 1968]. This passive conductance is the result of ion movements due to electric field effects caused by the active signal initiated near the axon hillock, the initial segment on the axon and initiation site of the action potential. These dendritic spikes seen extracellularly are initially positive going as ions are pushed out by electric fields induced from the inward current at the axon hillock [Holt, 1998]. Passive signals are reported to also incorporate low densities of voltage-gated ion channels that usually are not localized in high enough densities to induce active signal propagation [Meunier et al., 2002; Stuart et al., 1997].

Therefore, the characteristic signal of different cell compartments can be distinguished by the mechanism of firing (Figure 4). Passive dendrites respond with an initial positive current and active signals start with an initial negative current (Figure 5). It is known that special K^+ channels exist on dendrites to reduce the probability of active signals propagating up dendrites [Safronov, 1999]. It is not known if these K^+ channels are being expressed at the stage at which the cultures are dissected. In addition, the literature shows that different neurons express different voltage-gated ion channels, which can be distinguished by the action potential shape changes in response to specific pharmacological agents [Stuart et al., 1997].

In this thesis, I present the responses of these two types of AP shapes to various ion channel blockers: tetraethylammonium, 4-aminopyridine, and tetrodotoxin, as well as to the ionophor, monensin. AP shapes were studied using amplitudes and widths to determine concentration dependent responses. To my knowledge, this is the first categorical study of extracellular AP shapes and their responses to drugs recorded on microelectrode arrays.

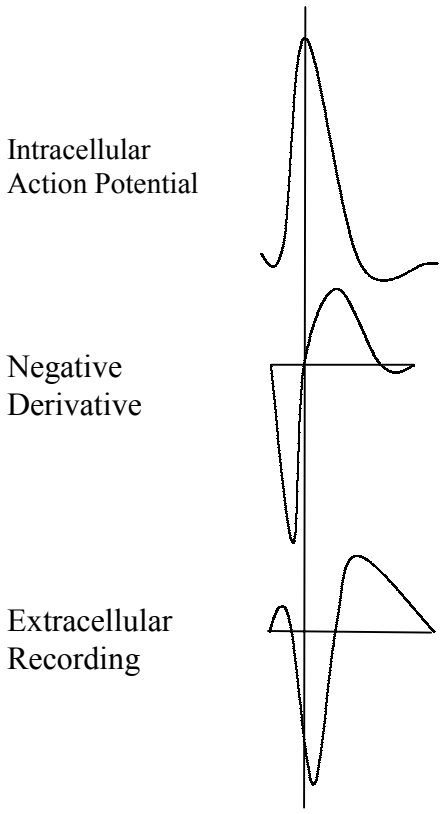

Figure 2: EXTRACELLULAR WAVESHAPE. Representation of data published by Henze et al. (2000) showing that the extracellular recording is the delayed derivative of the voltage in the action potential. Freygang and Frank (1959) explained that the delay is caused by the membrane capacitance.

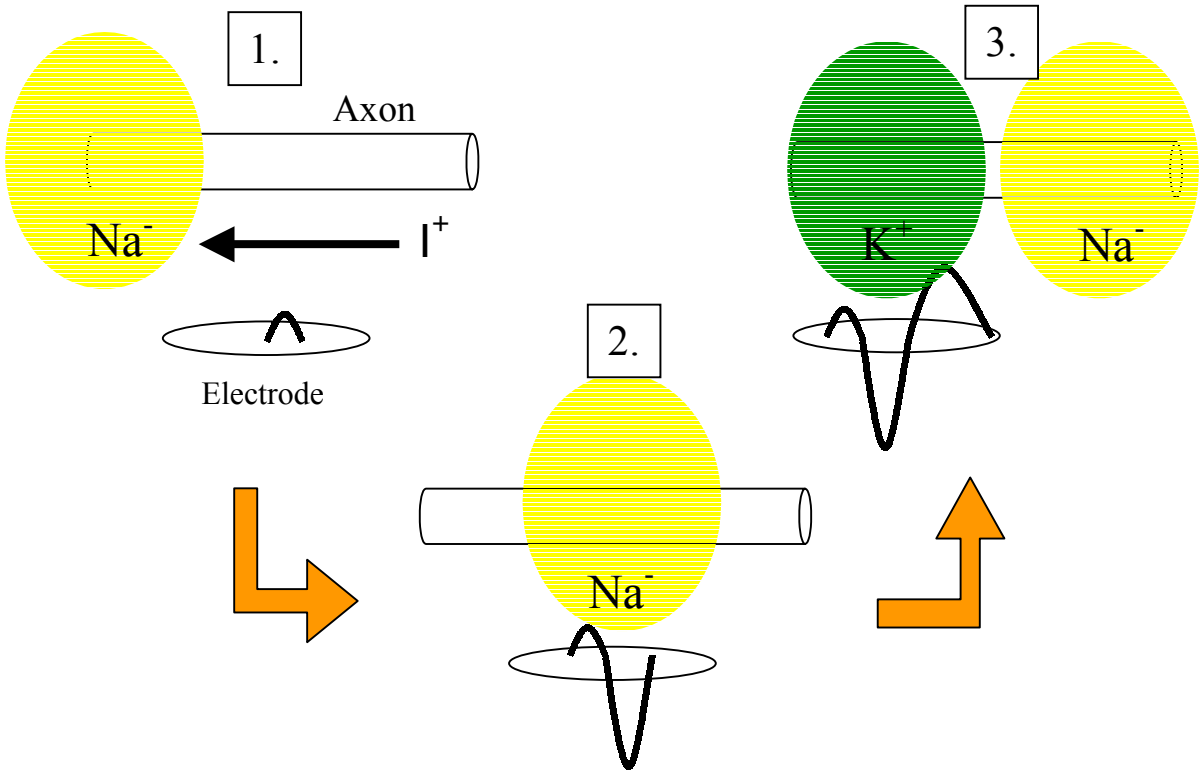

Figure 3: MECHANICS OF EXTRACELLULAR WAVESHAPE. Progress of active signal production. First, an initial positive current seen from the electrode is due to the displacement of positive ion currents as the Na depletion region (Na^-) approaches. Second, the large negative spike occurs as the Na^- region is directly above the electrode. Finally, the last positive peak comes from the K^+ hyperpolarizing current.

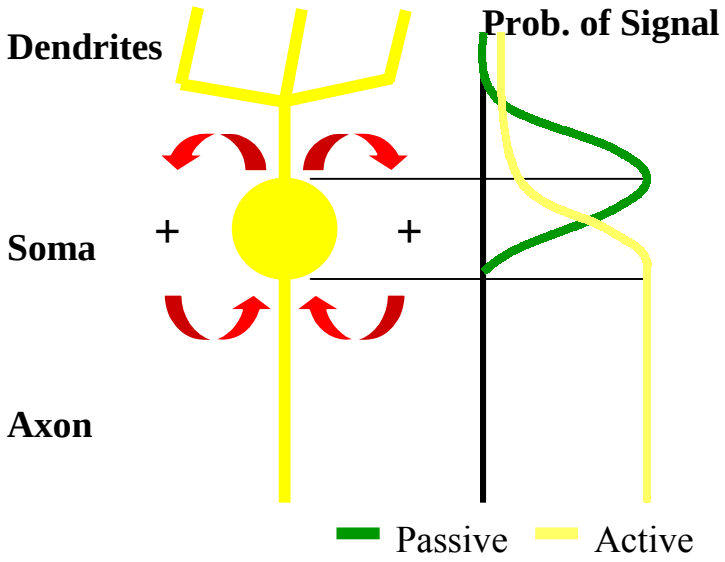

Figure 4: PASSIVE AND ACTIVE WAVESHAPES. Passive signals are the result of current pushed out as current flows in at the axon hillock. The highest probability of seeing a passive signal is at the base of the dendrite. The highest probability of seeing an active signal is in the axon and axon hillock. There is some probability of seeing an active signal in the dendrites.

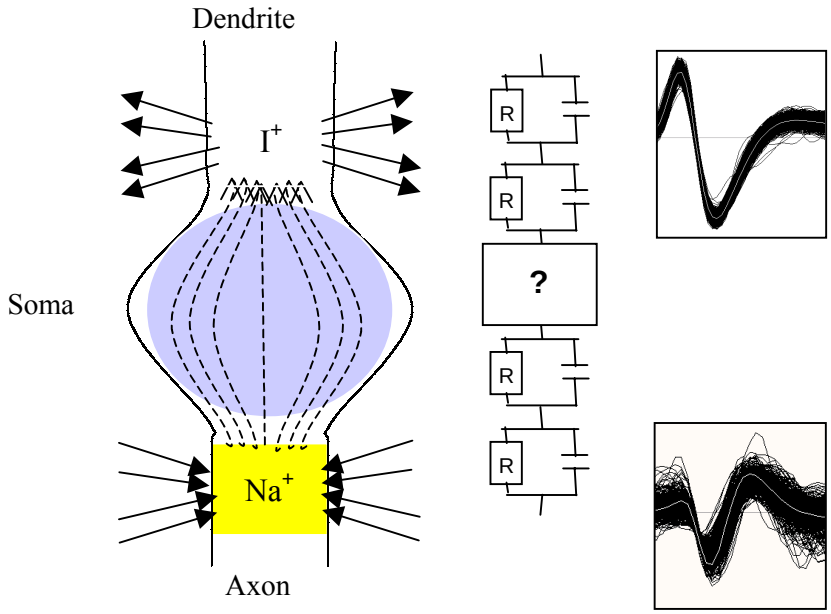

Figure 5: MECHANISM OF PASSIVE WAVESHAPES. Passive responses to action potentials are due to the electric fields (dashed lines) from charge entering the axon pushing ions out in the dendrites. The equivalent circuitry through the soma is unknown and undoubtedly complex; therefore, no particular relationship can be assumed.

2.3 General Theory of Voltage-gated Channels

The general theory of voltage-gated ion channels is complex. However, some general conclusions can be drawn which reveal the importance of ion channel distributions to understanding network states. It is important to make the distinction that voltage-gated sodium channels are important to determining membrane excitability [Waxman et al., 2000; Yu and Caterall, 2003]. Excitability is defined as the ease with which an action potential is initiated and ultimately, the upper limit on the firing rate of individual cells. Potassium channels, on the other hand, are important to shaping intrinsic firing properties such as bursting. For intracellular recordings, a burst is simply defined to be when a single stimulus results in a train of high frequency action potentials from a neuron (Waxman and Ritchie, 1985). The firing frequency within burst, the frequency of bursting, and the duration of bursts have been demonstrated to be strongly dependent on the kinetics of Na^+ and K^+ channels expressed – both voltage gated and Ca-dependent voltage gated (Baro et al., 2000; Harris-Warrick, 2002; Rashid et al., 2001).

In his Adrian lecture, Dr. Steve Waxman (1995) gave the following general points concerning ion channels:

1. Ion channels are distributed in a highly ordered fashion. Na^+ and fast K^+ channels have complementary distributions: the former segregated to the node of Ranvier and the latter to the paranodal region.
2. There are several different types of K^+ channels – fast, slow, etc. – that serve to modulate firing frequency and patterns.
3. There are several different types of Na^+ channels expressed in different types of axons.

2.3.1 Theory of Voltage-gated Na^+ Channels

There are, at the moment, nine voltage-gated Na channels that have been partially characterized by their pharmacology and histology [Novakovic et al., 2001]. Na_v 1.1, 1.2, and 1.3 are all TTX sensitive and found in the CNS. Na_v 1.4 and 1.5 are found in the skeletal muscle and heart respectively. Na_v 1.6 and 1.7 are TTX sensitive and found predominantly in dorsal root ganglion or in the CNS. Na_v 1.8 and 1.9 are TTX resistant and found in the DRG. However, this summary may not be complete since the dendrites of cerebullar purkinje cells are noted to TTX insensitive (Stuart et al., 1997). It should be noted that up to 12 Na_v channels have been postulated (Waxman et al., 1999).

The functional significance of specific Na channel types has been demonstrated in a recent study by Reganathan et al. (2003) on the expression of Na_v 1.8. Na_v 1.8 is normally expressed exclusively in the dorsal root ganglion and trigeminal ganglion neurons and not in the CNS. Purkinje cells predominately express only Na_v 1.1, 1.2, and 1.6. However, in the case of multiple sclerosis (MS) patients, histology reveals an upregulated expression of Na_v 1.8 in cerebellar Purkinje cells. Transfecting cerebellar Purkinje cells with Na_v 1.8 cDNA causes the following changes in action potentials and firing patterns:

1. increase in the amplitude and duration of action potentials;
2. reduction in the number of spikes within bursts;
3. increase in tonic, pacemaker-like impulse trains.

Therefore, both the shape of the action potential and the intrinsic firing properties are clearly linked to the expression of Na channels.

A further application of Na channel theory is in the area of pain, particularly for injured axons. Eccles et al. (1958) and Kuno and Llinas (1970) have reported the changes in somato-

dendritic spike production for axotomized motor neurons. This is due to disruption of axonal transport pathways. Waxman [1999] has also demonstrated that injury to the axons of dorsal root ganglion causes up regulation of TTX-resistant Na channels. This results in reduction of the firing threshold which allows for spontaneous firing as well as inappropriately high firing frequencies. These demonstrations reveal the importance of understanding ion channel functional significance to network states.

2.3.2 Theory of Voltage-gated K^+ Channels

The voltage-gated K^+ channel family is by far more diverse than Na^+ channels. Initial studies in *Drosophila* led to the identification of the K_v 1, 2, 3, and 4 families – *shaker*, *shab*, *shaw*, and *shal* families respectively. Mammalian studies revealed additional families of K_v 5, 6, 8, and 9 [Anderson and Greenberg, 2001]. Each family can have anywhere from one to six sub-types. Each subtype has its unique structure and kinetics and subtypes can form heteromers with new kinetic properties, which combine the properties of both. It is interesting to note that the evolutionary diversion of K^+ channel subtypes is the most ancient, appearing even in prokaryotes, whereas Na^+ channel diverge into only two subtypes for invertebrates with further diversion in vertebrates [Anderson and Greenberg, 2001].

Of course, before the molecular studies, pharmacological and electrophysiological studies had determined the existence of various types of K^+ channels and were given names according to their characteristic function. Safronov's review [1999] clearly details the distribution of these K^+ channels in the spinal dorsal horn. There are two types of fast, A-type K^+ channels. One is blocked by both 4-aminopyridine (4-AP) and dendrotoxin, and the other is blocked only by 4-AP. There is another type of delay-rectifier, K_{DR}, potassium channels or slow channels that are

sensitive to tetraethyl ammonium, TEA, but resistant to 4-AP [Safronov, 1999]. Waxman [1985] reports that in mature myelinated axons, the fast and slow K^+ channels are loosely co-localized, whereas fast K^+ channels are in the paranodal region and slow K^+ channels are distributed partially in the paranodal and partially in the node of Ravier. Finally, there are other families such as the inward-rectifying, K_{IR}, ATP-sensitive, and Ca^{2+}-dependent K^+ channels. All of these channels, particularly the Ca^{2+}-dependent type, have important effects on the firing patterns of neurons.

CHAPTER 3

METHODS

3.1 Microelectrode Array (MEA) Fabrication

The MEAs used were fabricated in house at the Center for Network Neuroscience (CNNS) as either a single array design with 64 multi-microelectrodes (MMEP 3), or a dual array design with 32 electrodes per matrix (MMEP 5). On the MMEP 5, two independent cultures with the same seeding date and derived from the same tissue can be monitored simultaneously and individually, each in their own medium bath. Electrodes are photoetched on 5 cm square sputtered indium-tin oxide (ITO) glass wafers, spin insulated with polysiloxane, cured, and laser de-insulated at the tips. Microelectrode recording sites have approximate diameters of 10 μm and are electrolytically gold-plated. Recording site impedance is about 1MΩ at 1 kHz. The MMEP insulation material is hydrophobic; surface activation and a hydrophilic adhesion island was generated by butane flaming at the center of the MMEP (Gross et al., 1985, Gross and Kowalski, 1991).

3.2 Cell Culture

Frontal cortex or spinal cord murine cultures were prepared from embryonic dissociated spinal cord (E14) or frontal cortex (E15.5) using the method of Ransom et al. (1977) slightly modified to include enzymatic digestion (Figure 7; Gross et al., 1997). Seeding concentrations were 5×10^5 cells/mL. Cultures begin producing spontaneous activity with coordinated bursting at around 21 days. All cultures used in this study were more than 27 days old. The care and use of, as well as all procedures involving, animals in the study were approved by the institutional

animal care and use committee of the University of North Texas and are in accordance with the guidelines of the Institutional Care and Use Committee of the National Institute on Drug Abuse, National Institutes of Health, and the *Guide for the Care and Use of Laboratory Animals* (Institute of Laboratory Animal Resources, Commission on Life Sciences, National Research Council, 1996). Mice were euthanized by means of CO_2 narcosis, followed by cervical dislocation.

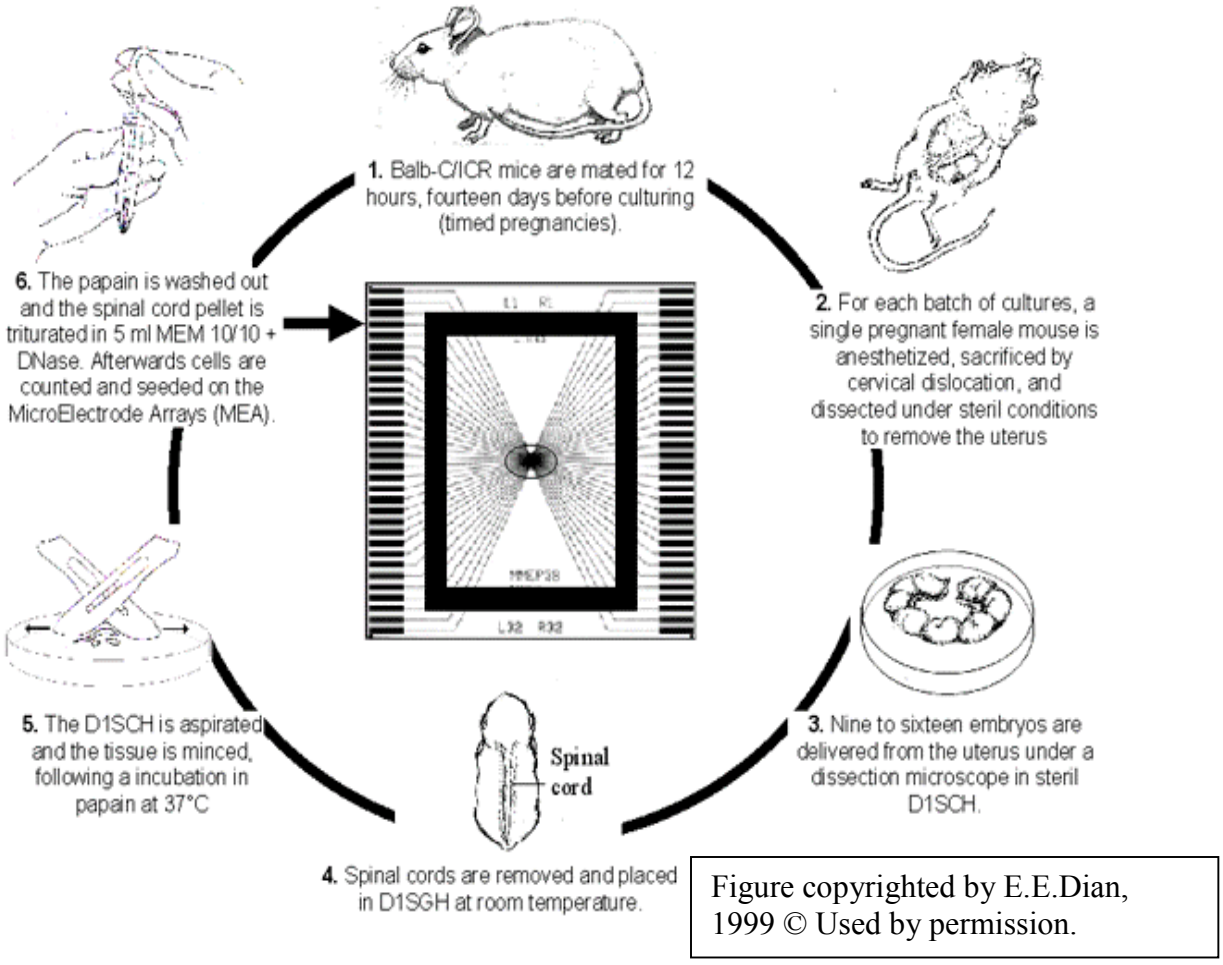

Figure 6: PREPARATION OF EMBRYONIC NEURONAL CULTURES. Summary of cell culture preparation plated on multielectrode arrays. Drawing by Emese Dian, CNNS Archive.

3.3. Recording Hardware

A Plexon Multichannel Acquisition Processor™ (MAP; Plexon Inc. Dallas TX) consisting of 64 two-stage amplifiers and analog-digital converters with a sampling rate of 40 kHz, and 32 digital signal processors (DSP's) was used for the recording. Zebra strips™ were used to connect the pre-amplifiers and electrode contacts on the MEA (Fujipoly America Corporation, Carteret, NJ). The total system gain was typically set at approximately 11K. Up to four units per channel can be discriminated based on their signal-to-noise ratios, usually between 2:1 and 20:1, using template-matching software (SortClient v. 1.21, Plexon Inc., Dallas TX). Hence, the system was capable of detecting and processing up to 128 discriminated units or neurons recorded from 32 electrodes.

3.4 Recording Environment

The cultures were placed on a heated base plate at 37^{o} C in bicarbonate buffered medium (spinal cord – modified Eagle's medium, MEM, with 10 % horse serum; frontal cortex – Dulbecco's modified Eagle's medium, DMEM, with 5 % horse serum) under a slow stream of humidified, 10% CO_2 (5-10 mL/min) to maintain a constant pH at 7.4. Stainless steel chambers, which contain the constant medium bath on the culture during recording, were sterilized by autoclaving before experiments. A minimum of 30 minutes of reference activity was recorded after culture medium was replaced by fresh stock. After the reference activity period, concentrations of the test compounds were added sequentially to the static bath (2 mL for MMEP 3; 1mL per well for MMEP 5) to raise the net concentration. Additional compound applications were made only after a stable activity (mean network spike rate) response was achieved. In the

case of ion channel modulators, many of the studies were completed under the effects of biccuculine in an effort to maintain higher activity and ensure that sufficient AP shape data could be collected. In the case of the gap junction blockers, cultures were used in multiple tested if it is found that, after a wash, the activity returned to the original reference state. Signals from the electrodes were recorded digitally at a 40 kHz sampling rate.

3.5 Statistical Analysis

In general, AP shapes consisted of a positive peak (peak 1), a negative peak (peak 2), followed by another positive peak (peak 3). Each unit was classified according to the shape of the extracellularly recorded AP into type I and type II (Figure 8). A small number of signals were excluded from the study due to inability to fit into the classification parameters. Type I AP shapes were defined to be when peak 3 had greater amplitude than peak 1. Type II AP shapes were defined to be when peak 3 had lesser amplitude than peak 1. The amplitude and width response of each peak were characterized for every neuron and classified into types and subpoputions. Subpopulations were defined using the criteria of whether a significant increase, decrease, or no change was observed for peaks 1, 2, or 3 at various drug concentrations. Significance for this thesis is determined using the Student's t-test. T-tests were used by including 20 to 30 minutes of native activity for each unit and comparing this to 20 to 30 minutes of activity during the manipulation by drug or temperature. Averaged network responses, subpopulation densities, and intra-cultural variations were determined using averages and standard deviations. All results were compared to *in vivo* measurements, if available, as reported in literature, with special emphasis placed on specific subpopulation responses and effective concentration ranges.

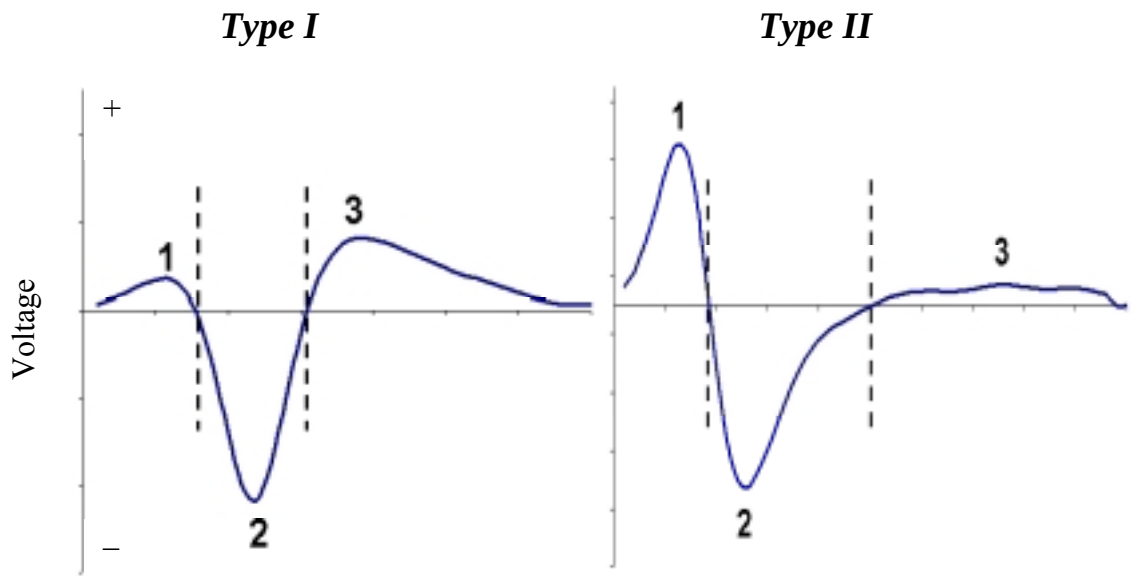

Figure 7: TYPE I AND TYPE II SIGNALS. Classification of extracellularly recorded signals based on the shape of the signal. Every signal consists of a positive peak (peak 1), followed by a negative peak (peak 2), and a second positive peak (peak 3). Type I: peak 3 is larger than peak 1. Type II: peak 3 is smaller than peak 1. Type I represents active signal propagation; and, type II represents passive dendritic signal.

3.6 Software Development

Software was developed in order to handle the large datasets. The first software, plxread.exe, read the recorded data file and outputs AP shapes from each recorded unit, averaged in minute bins, to text files. Next, MS Excel™ macros, WaveAnalyzerc.xla, was written to: identify peaks; measure amplitudes and widths; plot AP shapes and amplitudes; measure averaged amplitude and width responses for each experiment episode; establish significance of responses with student t-tests; sort responses based on AP shape type – type I and type II;

calculate whole network, type I, and type II averaged changes; plot concentration response curves. The code for this software is included in Appendix A.

CHAPTER 4

RESULTS

4.1 Temperature Studies

A classical study to demonstrate the action of ion channels for intracellular recording uses temperature because the kinetics of the channels slows with reductions in temperature. This attenuates and broadens AP shapes. The response of extracellular action potentials to changes in temperature were measured for two steps, $\Delta T = 5$ °C and $\Delta T = 10$ °C. In both cases, dramatic changes in amplitude and width were observed (Figure 9). Responses classified as increases or decreases were determined using the t-tests. Most of the amplitudes of type I signals decreased with temperature, however a surprising 29.8 % and 34.9 % of neurons increased for 5 °C and 10 °C steps respectively (Tables 1 and 2). The averaged percent change for peak 2 of type I was 2.9 % for $\Delta T = 5$ °C and 8.5 % decrease for $\Delta T = 10$ °C. For peak 3 of type I, the average change was a 2.4 and 2.3 % increase for the same changes in temperature. Almost all AP shapes increased the full width at half maximum (FWHM) for peak 2 in response to temperature decreases. The average peak 2 width change was an 11.8 and 33.7 % increase for $\Delta T = 5$ °C and 10 °C respectively. Less than 3 % of AP shapes showed no change to temperature. In the case of type II, n was very small (n = 3) and the AP shapes also showed decrease in amplitude and increase in width.

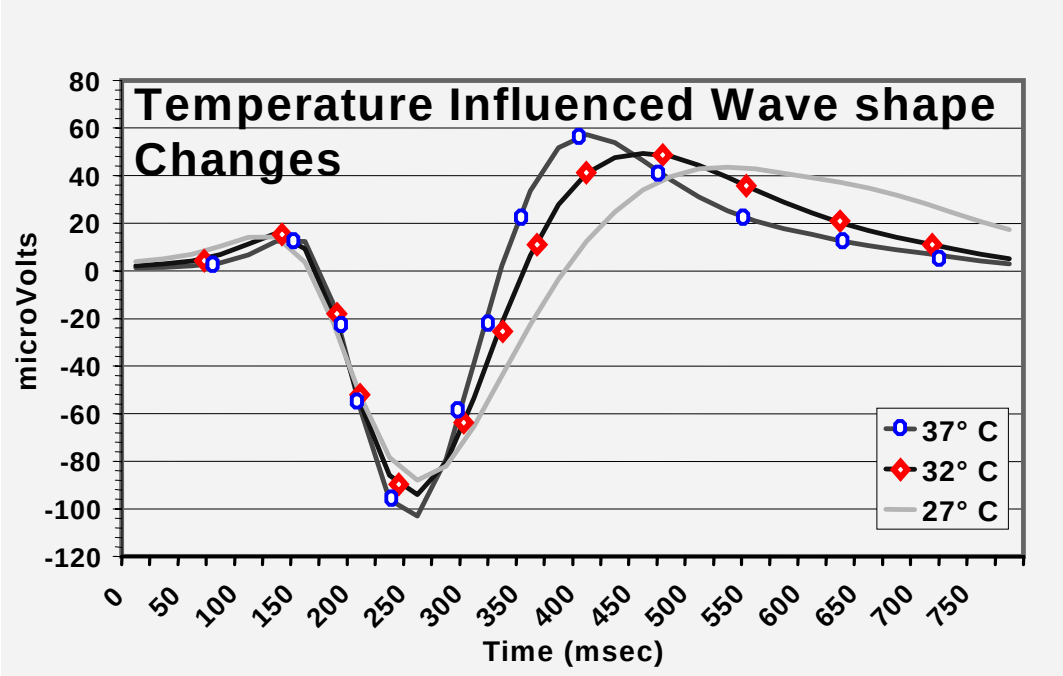

Figure 8: TEMPERATURE EFFECTS ON WAVESHAPES. Changes in AP shape for a type I AP shape in response to temperature.

Type I	Peak 2	Peak 3	FWHM	Type II	Peak 1	Peak 2	FWHM
Increase	10.6	29.8	93.6	Increase	---	---	100.0
Decrease	44.7	44.7	4.2	Decrease	66.7	33.3	---
No Change	44.7	25.5	2.1	No Change	33.3	66.7	---

Table 1: Percent of neurons that changed in response to a 5 °C change in temperature ($n_{TI} = 47$, $n_{TII} = 3$). FWHM refers to the full width at half maximum for peak 2.

Type I	Peak 2	Peak 3	FWHM	Type II	Peak 1	Peak 2	FWHM
Increase	9.3	34.9	100.0	Increase	---	---	100.0
Decrease	74.4	44.1	---	Decrease	100.0	100.0	---
No Change	16.2	20.9	---	No Change	---	---	---

Table 2: Percent of neurons that changed in response to a 10 °C change in temperature ($n_{TI} = 43$, $n_{TII} = 3$). FWHM refers to the full width at half maximum for peak 2.

4.2 Pharmacological Studies

4.2.1 Tetraethylammonium (TEA)

Tetraethylammonium is a slow K^+ channel blocker causing attenuation of peak-to-peak amplitudes and prolongation of action potentials in nonmylenated neurons [Nashmi and Fehlings, 2001; Bostock et al., 1981]. TEA was applied to three murinal spinal cord cultures (49, 28, and 34 DIV) with the following concentration ranges: 0.1 to 1.4 mM, 0.3 to 3.4 mM, and 0.3 to 4.0 mM (Figure 10 and 11). The hypothesis for these tests was that the third peak of type I neurons would decrease since that is the peak dependent on K^+ currents. A total of 129 neurons were recorded with 87 Type I (67 %) and 42 Type II AP shapes (33 %). The median amplitudes for the signals are summarized in Table 3.

For peak 2 there were three subpopulation responses (Table 4): (1) 17.4 ± 15.3 % of Type I neurons in each culture increased ($p < 0.05$) in amplitude, (2) 34.4 ± 18.6 % decreased ($p < 0.05$), and (3) 44.1 ± 3.9 % showed no significant change ($p > 0.05$). Peak 3 of Type I AP shapes showed a gradual and significant dose dependent amplitude decrease ($p << 0.05$ at 4.0 mM). For peak 3 there three subpopulations were (1) 15.2 ± 13.7 % of Type I neurons in each culture increased, (2) 58.9 ± 24.6 % decreased, and (3) 23.8 ± 9.6 % showed no change. For those whose decreased in peak 3 of type I, the decrease was 22 ± 14 % at 1.4 mM, 31 ± 18 % at 3.4 mM, and 33 ± 18 % at 4.0 mM. Of the Type I signals, eleven AP shapes (13 %) no change whatsoever to TEA. The extrapolated EC50 for the decrease in Peak 3 of Type I calculated from the averaged net response was 18.8 mM TEA, however cultures would not be spontaneously active at this high concentration. In Type II AP shapes, the first peak did show varying decreases in amplitude (ranging 5 to 20 %) and the second peak did not display consistent amplitude changes.

	JS013 (μV)	JS014 (μV)	JS016 (μV)
Type I Peak 1	10.1 ± 11.2	4.4 ± 14.7	17.6 ± 22.8
Type I Peak 2	- 46.1 ±13.1	-44.6 ± 36.7	-84.3 ± 64.1
Type I Peak 3	20.7 ± 13.8	17.3 ± 27.4	52.2 ± 45.1
Type II Peak 1	32.5 ± 51.3	39.2 ± 65.1	57.1 ± 49.7
Type II Peak 2	- 54.8 ± 44.6	-53.6 ± 61.7	-64.2 ± 27.5
Type II Peak 3	13.5 ± 10.2	9.1 ± 8.0	18.8 ± 9.7

Table 3: The median amplitudes and standard deviations of each peak for the three spinal cord cultures used in measuring amplitude response to TEA. Recordings are from 87 type I and 42 type II signals.

Tetraethyl ammonium – Spinal Cord Response (SC)

	Type 1 Peak 2	Type 1 Peak 3	Type 2 Peak 1	Type 2 Peak 2
Increase	17.4 ± 15.3 %	15.2 ± 13.7 %	7.1 ± 10.1 %	7.1 ± 10.1 %
Decrease	34.4 ± 18.6 %	58.9 ± 24.6 %	71.4 ± 20.2 %	57.1 ± 0.1 %
No Change	44.1 ± 3.9 %	23.8 ± 9.6 %	21.4 ± 30.1 %	21.4 ± 30.1 %

Table 4: Percentage of neurons to responsding to tetraethyl ammonium. Increases and decreases were determined using t-tests ($p < 0.05$) comparing the amplitude during the native activity to the amplitude at maximum concentration of TEA.

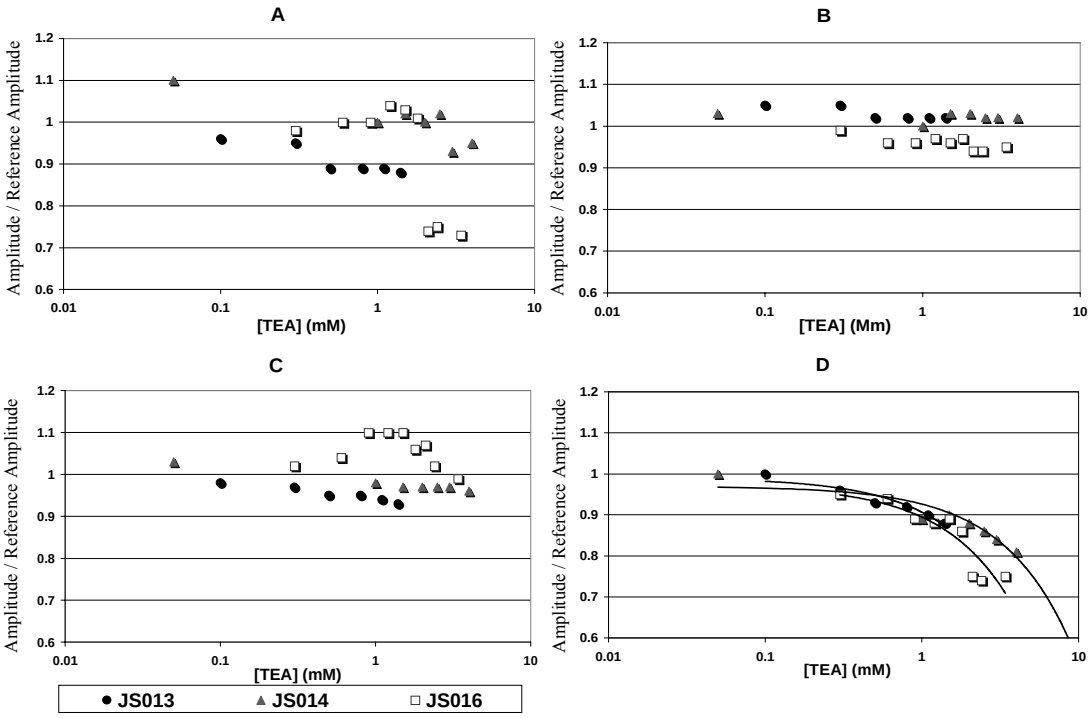

Figure 9: CONCENTRATION RESPONSE TO TETRAETHYL AMMONIUM.

Concentration responses [0.05 – 4.0 mM] to tetraethylammonium in mouse spinal cord culture. AP shape amplitude changes were measured using three separate cultures: JS013 (49 DIV; n = 29), JS014 (28 DIV; n = 41), and JS016 (34 DIV; n = 59). Figures A thru C show the response for peak 1 of type II, peak 2 of type I, and peak 2 of type II. In Figure D, the third peak of Type I shows a significant and dose dependent decrease in amplitude ($p << 0.5$ at 4.0 mM). The average EC50 for the third peak of the Type I waveforms is 18.8 mM (SD = 15.2).

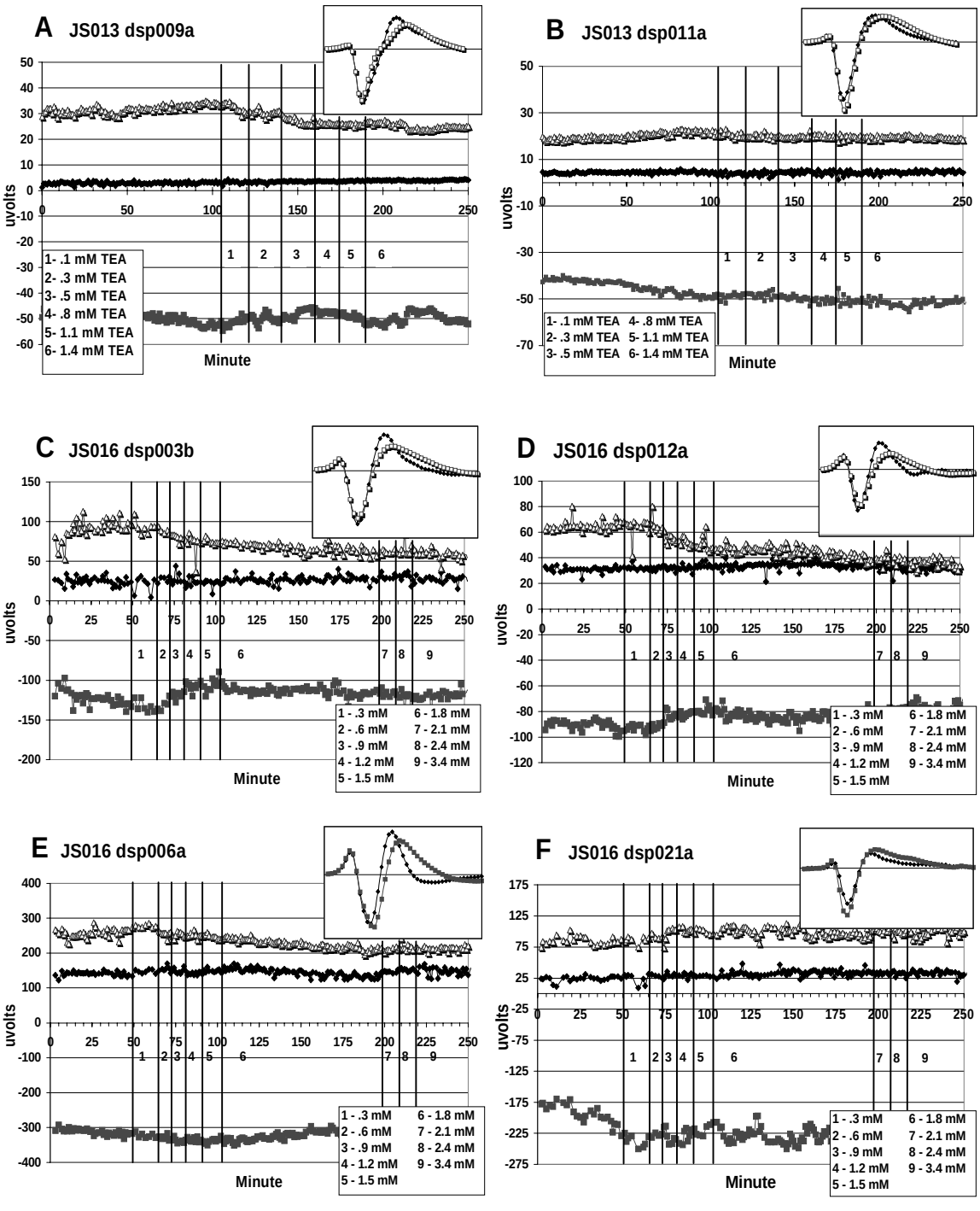
A JS013 dsp009a
uvolts
Minute
1- .1 mM TEA
2- .3 mM TEA
3- .5 mM TEA
4- .8 mM TEA
5- 1.1 mM TEA
6- 1.4 mM TEA
B JS013 dsp011a
uvolts
Minute
1- .1 mM TEA 4- .8 mM TEA
2- .3 mM TEA 5- 1.1 mM TEA
3- .5 mM TEA 6- 1.4 mM TEA
C JS016 dsp003b
uvolts
Minute
1 - .3 mM 6 - 1.8 mM
2 - .6 mM 7 - 2.1 mM
3 - .9 mM 8 - 2.4 mM
4 - 1.2 mM 9 - 3.4 mM
5 - 1.5 mM
D JS016 dsp012a
uvolts
Minute
1 - .3 mM 6 - 1.8 mM
2 - .6 mM 7 - 2.1 mM
3 - .9 mM 8 - 2.4 mM
4 - 1.2 mM 9 - 3.4 mM
5 - 1.5 mM
E JS016 dsp006a
uvolts
Minute
1 - .3 mM 6 - 1.8 mM
2 - .6 mM 7 - 2.1 mM
3 - .9 mM 8 - 2.4 mM
4 - 1.2 mM 9 - 3.4 mM
5 - 1.5 mM
F JS016 dsp021a
uvolts
Minute
1 - .3 mM 6 - 1.8 mM
2 - .6 mM 7 - 2.1 mM
3 - .9 mM 8 - 2.4 mM
4 - 1.2 mM 9 - 3.4 mM
5 - 1.5 mM

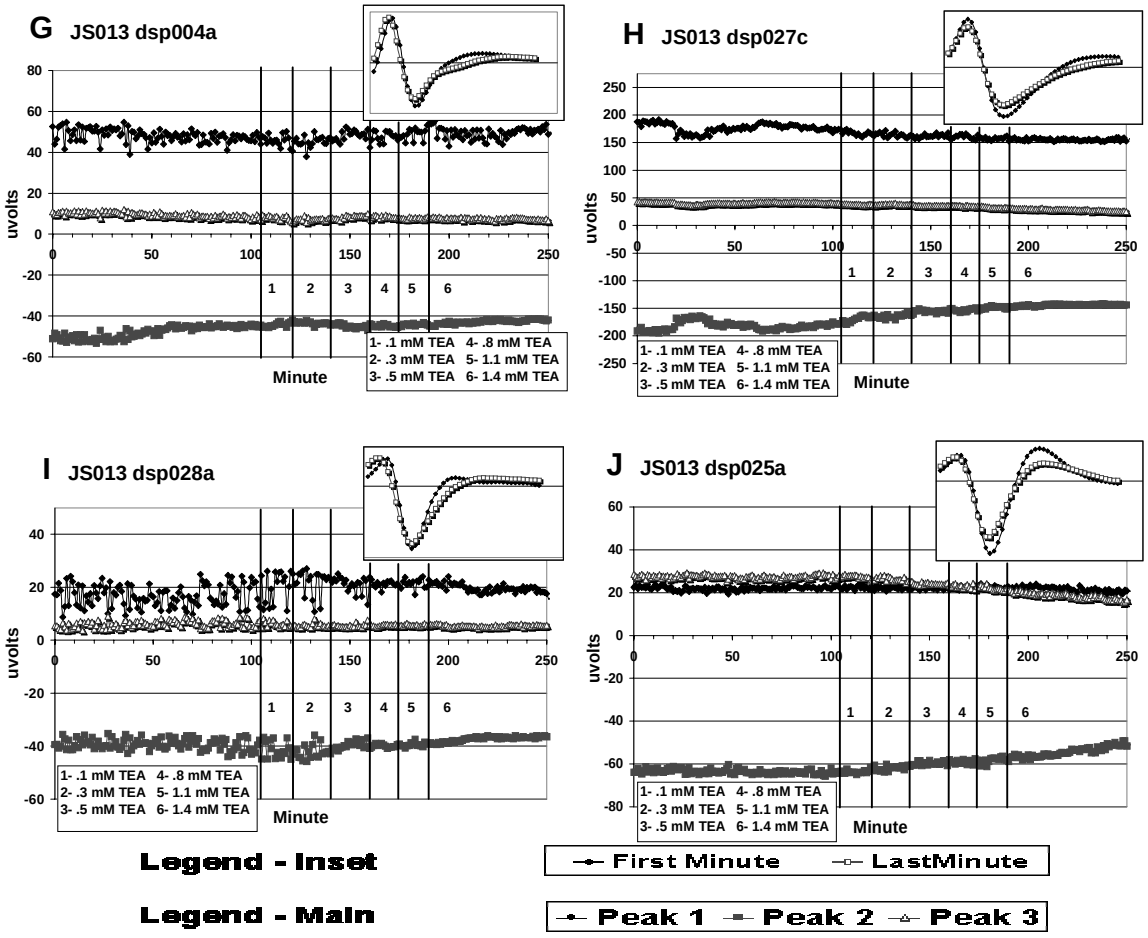

Figure 10: TETRAETHYL AMMONIUM EFFECTS. Temporal evolution of peak amplitude change as a function of concentration of TEA. A) A typical type I dose dependent decrease. B) An increase in peak 2 and broadening of peak 3. C & D) A decrease and broadening of peak 3 for type I signals. E) Broadening of peaks 2 and 3 for type I. F) Increase in amplitude for type I. G) Modification of peak 3 for type II. H) Decrease in amplitude for type II. I) Broadening of type II signal. Initial fluctuations of peak 1 are of unknown origins and were not noticed in other units. J) Switch from type I to type II for a unit after drug application. In most instances, switching occurred spontaneously without drug application (See section 4.7).

Not all neurons responded in the same manner to increasing TEA concentration: some decreased, some increased, or showed no change. A subpopulation analysis was performed to study any correlation between those neurons that show a significant or no significant change. For Type II, it was found that no noticeable trend existed for the percentage of type II neurons showing a significant increase, decrease, or no change in each peak. However, as expected, there was more acute decrease in amplitude in peak 3 of Type I neurons for the subpopulation of Type I signals showing a significant decrease in peak 3 (Figure 12). No Type I signal showed a significant increase in peak 3 to TEA at 4.0 μM. Also, in general the average full width at half-maximum for the negative peak (peak 2) of type II increased in a dose dependent manner by approximately 20 % at 4 mM TEA (data not shown). For the widths for peak 2 in Type I / Type II, 20.8 ± 10.5 % / 21.4 ± 10.1 % of neurons in each culture increased, and 20.4 ± 6.4 % / 14.3 ± 20.1 % decreased. Also, 53.9 ± 13.9 % of neurons per culture increased in width of peak 3 for Type I neurons.

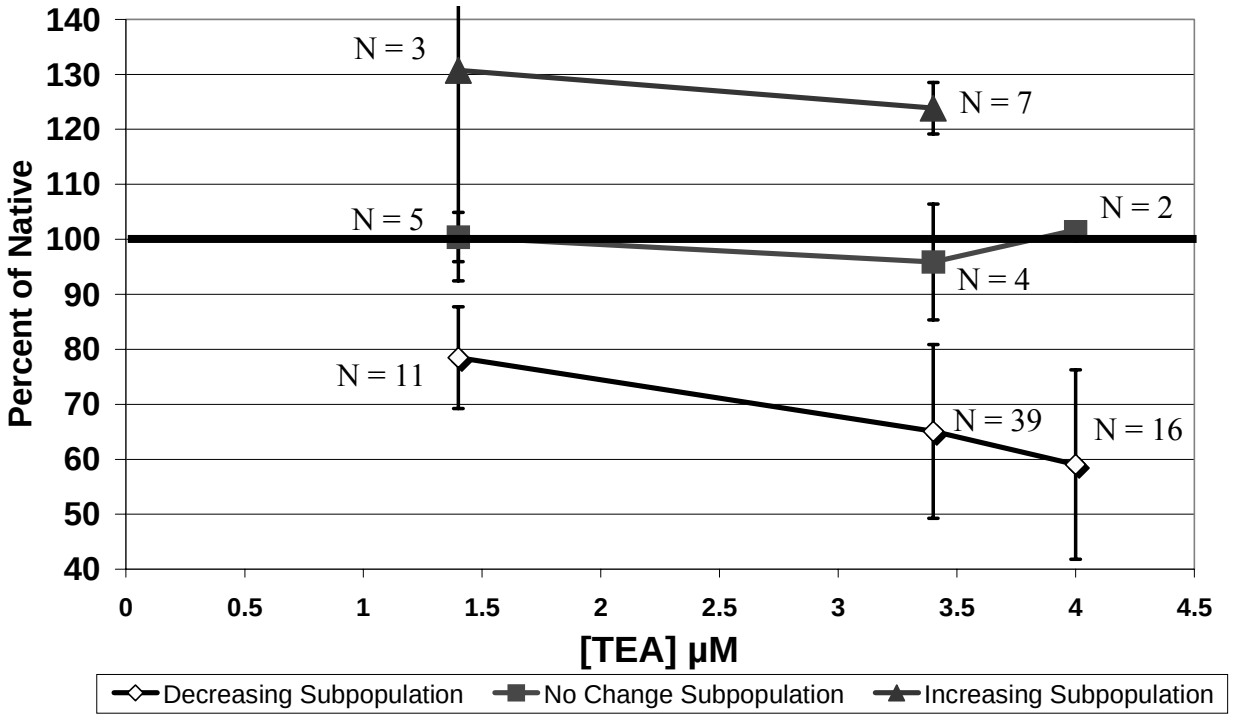

Figure 11: SUBPOPULATION ANALYSIS UNDER TETRAETHYL AMMONIUM. Subpopulation concentration response curves for type I peak 3 signals. A steeper response of peak 3 to TEA was seen for the subpopulation of signals showing a significant decrease in peak 3. There were no signals increasing from TEA at 4.0 µM concentration. The total number of signals from three different cultures at 1.4 µM was 19, at 3.4 µM was 50, and at 4.0 µM was 17.

4.2.2. 4-Aminopyridine (4-AP)

4-AP, another voltage-gated potassium channel blocker, was applied to two frontal cortex cultures (36 and 27 DIV) with concentration ranges from 0.05 to 1.0 mM. In this case, 67 neurons were recorded with 55 Type I (82 %) and 12 Type II AP shapes (18 %). The hypothesis for these tests are again that the third peak of type I will decrease demonstrating the K^+ channel involvement. The negative peak of Type I showed only small and conflicting decreases. Results for subpopulation responses are summarized in Table 5 for 4-AP. For this peak, 44.5 ± 13.0 %

decreased, 20.8 ± 12.2 % increased, and 34.7 ± 0.8 % showed no change. However, Peak 3 of Type I showed a sudden significant decrease (Figure 13) upon initial application of 4AP followed by a gradual decrease with concentration ($p << 0.05$ at 1.0 mM). The average decrease for peak 3 was 19.6 % or a 28 ± 18 % decrease for the subpopulation of decreasing type I signals (Table 5). For peak 3, 70.7 ± 0.1 % decreased, 17.4 ± 0.4 % increased, and 12.0 ± 0.3 % showed no change. Four of the Type I AP shapes (7 %) did not respond to the 4AP.

The first peak of Type II AP shapes also showed a sudden 25 percent decrease, whereas peak 2 of Type II showed a small (< 8%) and inconsistent decrease (data not shown). For Type II peak 1 / peak 2, 62.5 ± 53.0 % / 58.3 ± 11.8 % showed a decrease, 25.0 ± 35.4 % / 0.0 ± 0.0 % increased, and 12.5 ± 17.7 % / 41.7 ± 11.8 % showed no change (Table 5). For the widths, the average half-max width increase was greater than 10 % (note: due to window size limitations, this could not be measured accurately). For peak 2 of Type I, 56.4 ± 13.3 % increased and 17.6 ± 25.0 % decreased. In peak 3 of Type II, 60.1 ± 18.4 % increased (Table 5).

4-aminopyridine – Neuron Response (FC)

	Type 1 Peak 2	Type 1 Peak 3	Type 2 Peak 1	Type 2 Peak 2
Increase	20.8 ± 12.2 %	17.4 ± 0.4 %	25.0 ± 35.4 %	0.0 ± 0.0 %
Decrease	44.5 ± 13.0 %	70.7 ± 0.1 %	62.5 ± 53.0 %	58.3 ± 11.8 %
No Change	34.7 ± 0.8 %	12.0 ± 0.3 %	12.5 ± 17.7 %	41.7 ± 11.8

Table 5: Percentage of neurons to response to 4-aminopyridine. Increases and decreases were determined using t-tests ($p < 0.05$) comparing the amplitude during the native activity to the amplitude at maximum concentration of 4-AP.

JS017 – 1.0 mM

Type	P2 PERCENT CHANGE	P3 PERCENT CHANGE
Type II (N=7)	-2.2 ± 27.3	-103.5 ± 188.0
Type I (N=38)	8.6 ± 20.6	22.6 ± 43.5
Total (45)		

JS018 – 1.0 mM

Type	P2 PERCENT CHANGE	P3 PERCENT CHANGE
Type I (N=17)	-0.6 ± 12.0	-12.8 ± 26.3
Type II (N=5)	-10.3 ± 14.1	-3.6 ± 79.3
Total (22)		

Table 6: Summary of changes due to 4-AP from two experiments, showing a mean percent decrease 22.6 and 12 .8 % for type I peak 3 in response to 1.0 mM 4-AP. Note that peak 2 is minimally effected.

(Next Page) Figure 12: 4-AMINOPYRIDINE EFFECT. Temporal evolution of peak amplitude change in type I and type II as a function of concentration of 4-AP. At 0.05 mM, a sharp amplitude decrease is seen in peak 3 and a gradual decrease in some units for peak 2 of a Type I AP shape under 4AP [0.05 – 1.0 mM]. Two cultures are represented, JS017 (36 DIV) and JS018 (27 DIV). (A) Sharp decrease in type I for peaks 2 and 3 and an increase in peak 1. (B) Sharp decrease in all peaks of type I and a broadening of the AP shape. (C) No change in amplitude of type I but a broadening of the AP shape. (D) No change in type I can be observed within the window of recording. (E) Sharp decrease in peak 3 and gradual decrease of peak 2 for type I. (F) Sharp decrease in peaks for type II. (G) Slight increase in type II. (H) Large increase in type II.

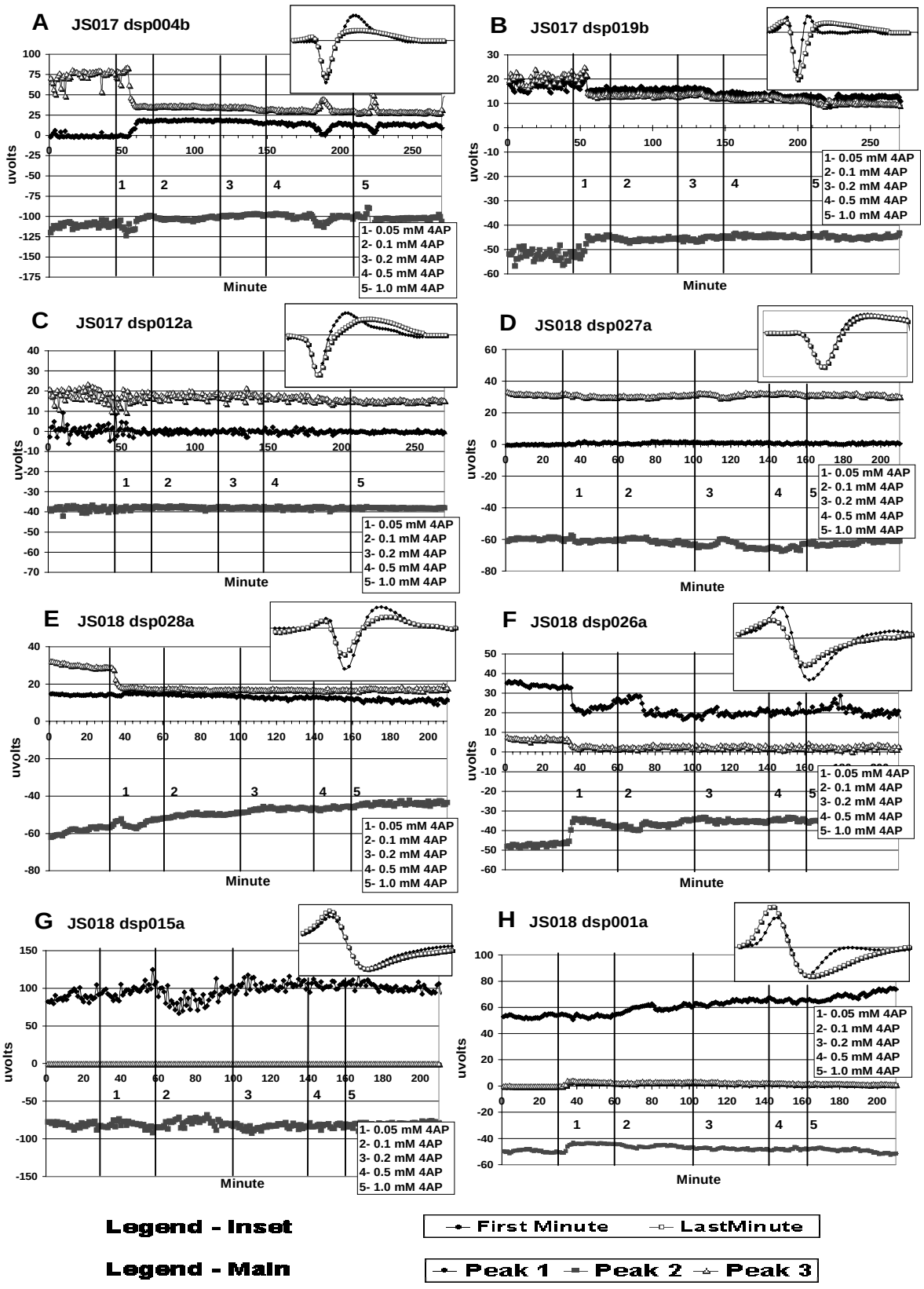
A JS017 dsp004b
B JS017 dsp019b
C JS017 dsp012a
D JS018 dsp027a
E JS018 dsp028a
F JS018 dsp026a
G JS018 dsp015a
H JS018 dsp001a
uvolts
Minute
1- 0.05 mM 4AP
2- 0.1 mM 4AP
3- 0.2 mM 4AP
4- 0.5 mM 4AP
5- 1.0 mM 4AP
Legend - Inset
First Minute
LastMinute
Legend - Main
Peak 1
Peak 2
Peak 3

4.3 Monensin

Initial attempts to measure sodium current contributions to the AP shape were made using tetrodotoxin. However, spontaneous activity of the network was eliminated at a 25 nM concentration before any appreciable change in the AP shape occurred. Published concentrations used to demonstrate significant blocking of sodium currents are on the order of 300 nM (Hille, 1992).

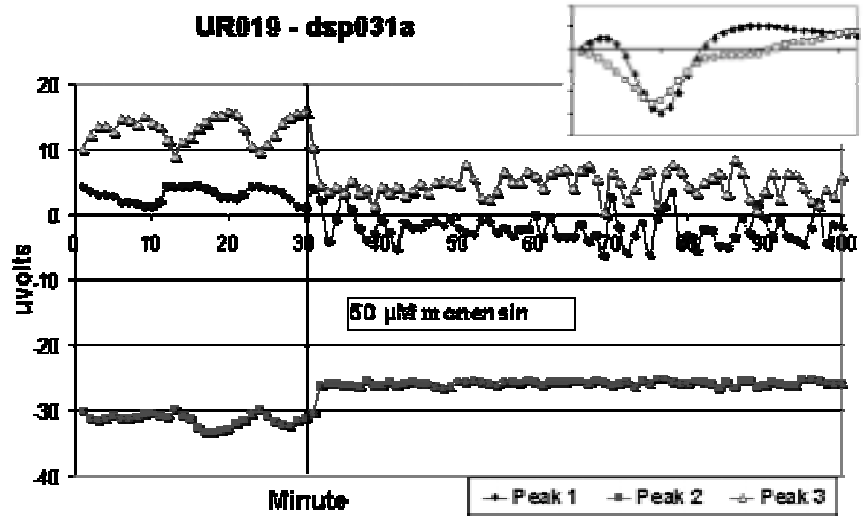

Figure 13: MONENSIN EFFECT. Response of a selected unit to monensin. Only a subpopulation of 58 % showed a significant decrease in peak to peak amplitude – one of the largest being displayed here.

Monensin, a Na^+ ionophore, was applied to two mouse spinal cord cultures (47, and 26 DIV) at a series of concentrations [5, 20, and 50 µM]. A total of 67 neurons were recorded from with 41 Type I (68 %) and 19 Type II AP shapes (32 %). It was anticipated that the negative peak (peak 2) of Type I AP shapes would decrease in amplitude in response to the reduction of the membrane potential caused by the monensin-induced sodium permeability. Over all, the average decrease of all Type I AP shapes was negligible at all concentrations (data not shown).

However, subpopulation analysis showed significant decreases in 24 of the 41 (58 % of units) Type I (Figure 14; $p << 0.05$ at 50 μM). For Type II neurons, the average response was also negligible, but 11 of the 19 units (58 % of units) also showed a significant decrease of peak 2 amplitude ($p < 0.05$ at 50 μM).

4.4 General Developmental Studies

Studies were conducted to measure the changes in AP shape amplitudes and types over weeks in vitro for spinal cord tissue. Three to four spinal cord cultures were selected from each of the ages of 3 (n = 3), 4 (n = 4), 5 (n = 4), and 7 (n = 4) weeks in vitro (WIV) (Table 7). In general, the average number of units per culture increased with age from weeks 3 through 7 (Figure 15). Also, it was found that the percentage of active signals generally decreased with age from 71 %, to 66 %, 77 %, and 64 %. Week 5 did not fit the general trends. The percentage of active signals in spinal cord was, in general, found to be lower (AVE = 65 %, n = 15) than in frontal cortex (AVE = 80 %, n = 3). There were no noticeable differences or trends in activity through these weeks.

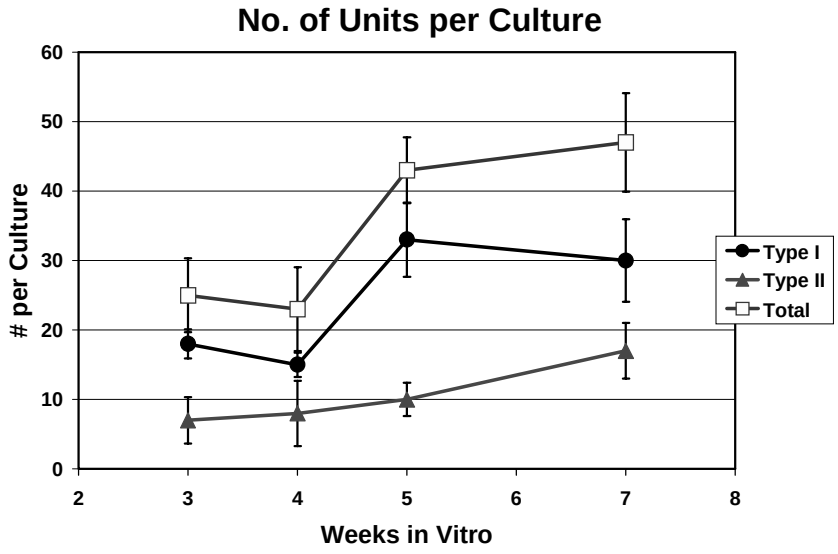

Figure 14: NUMBER OF UNITS PER CULTURE OVER TIME. The total number of units recorded with greater than 2:1 signal to noise ratios per culture increases with age from weeks 3 through 7. The number of type I neurons per culture had the largest increase between weeks 4 and 5 whereas the number of type II neurons increased steadily with age.

Experiment Name	Days In Vitro	Number of Type I	Number of Type II
ED174	26	17	3
ED013	26	15	5
JS020	26	22	14
JS014	28	19	22
ED172	32	17	2
ED178	33	14	5
ED014	33	11	3
JS016	34	48	7
JS021	35	29	5
ED113	40	35	13
ED111	41	23	15
ED029	48	35	16
JS013	49	24	28
JS022	54	17	9
ED030	56	44	14
Total		370	161

Table 7: Summary of data from CNNS archive used in development study. Fifteen neurons were excluded from the study because they could not be categorized as type I or type II.

4.5 Developmental Changes to Type I Signals

The most noticeable change in type I, active signals was the increase in the number of units from and average of 18 per culture to 30 per culture. Also, it was found that the amplitude of the signals increased with age (Figure 16). The average amplitude of the negative peak (P2) increased from 53 μV, to 63, 63, and 108 μV for weeks 3, 4, 5, and 7. For the positive peak 3 (P3), the average amplitude increased from 30 μV, to 31, 39, and 59 μV. The standard deviations of the first positive peak was very high (range varied > 75 %), however, the first peak also showed an increase on average with age from 11 μV, to 12, 13, and 25 μV for weeks 3, 4, 5, and 7.

The raw amplitudes of signals are directly dependent on both the current through the membrane and also the cell/ electrode geometry. For example, as the distance between the cell and the electrode increases, the amplitude of the signal would naturally decrease as a function of $1 / R^2$. However, since the dependence is direct, it follows that the effect can be normalized out of the equation by taking the ratio of the peak amplitudes. For each week, a non-normal distribution of peak 3 to peak 2 ratios was observed that varied only slightly but significantly from week to week with the peak at peak 3 being at a little less than 40 % of peak 2 (Figure 17; Kruskal-Wallis test, $p = 0.0007$).

(Next page) Figure 15: PEAK AMPLITUDE HISTOGRAMS. Distribution of peak 2 amplitudes for type I signals from weeks 3, 4, 5, and 7. Whereas the peak of the distribution does not change appreciably, the emergence of large amplitude signals in later weeks raises the average amplitude throughout development.

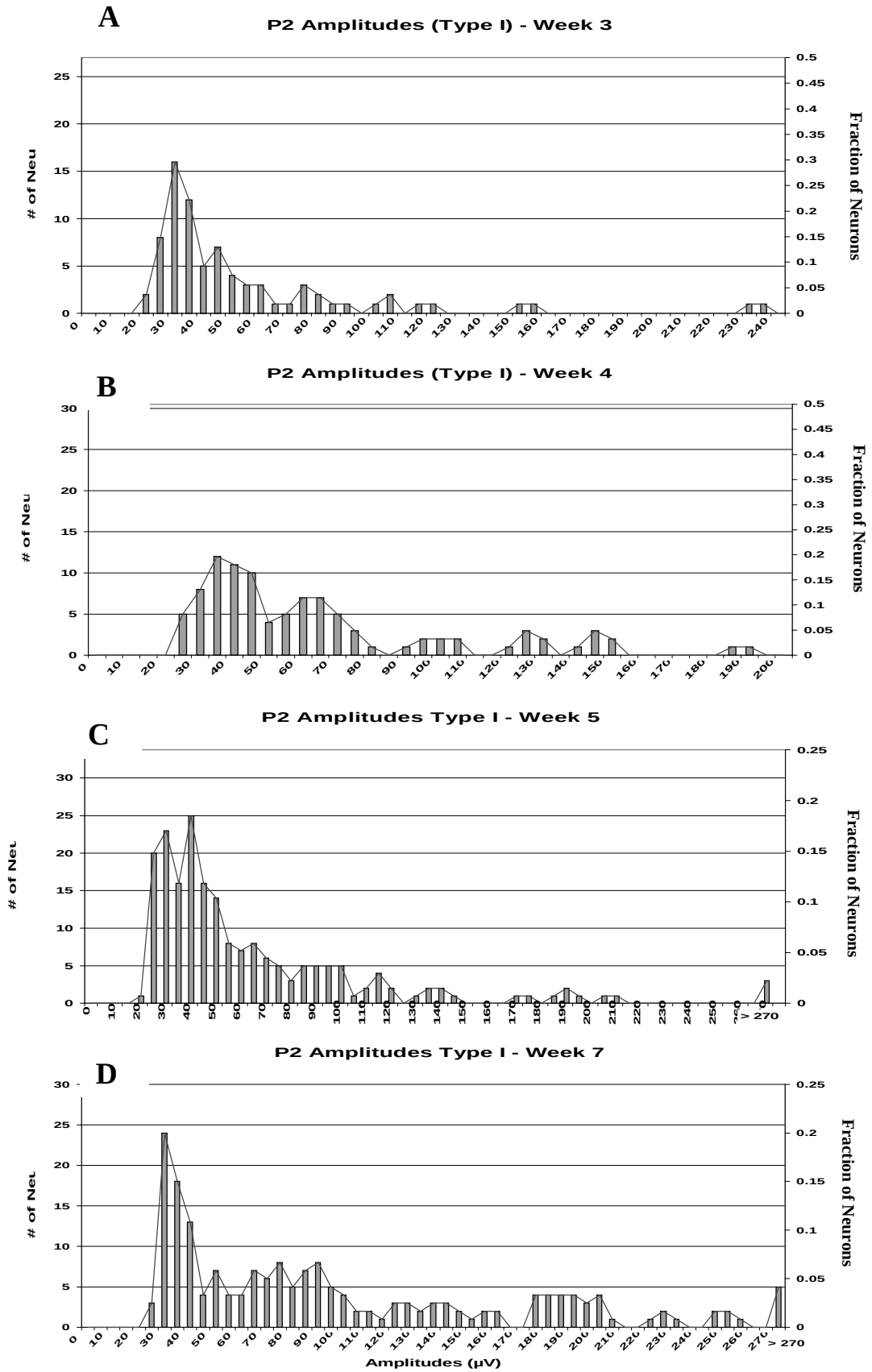
A
P2 Amplitudes (Type I) - Week 3
# of Neu
Fraction of Neurons
B
P2 Amplitudes (Type I) - Week 4
# of Neu
Fraction of Neurons
C
P2 Amplitudes Type I - Week 5
# of Neu
Fraction of Neurons
> 270
D
P2 Amplitudes Type I - Week 7
# of Neu
Fraction of Neurons
> 270
Amplitudes (μV)

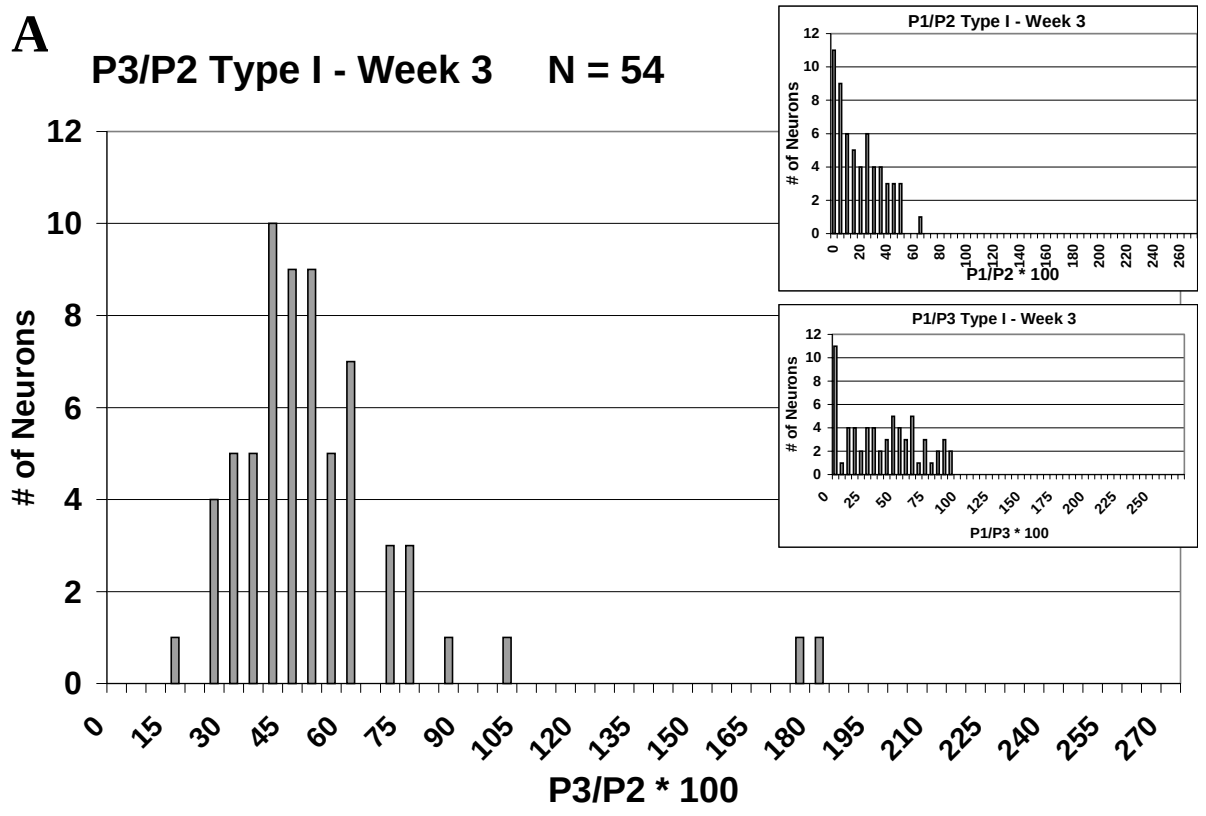
A
P3/P2 Type I - Week 3 N = 54
# of Neurons
P3/P2 * 100
P1/P2 Type I - Week 3
# of Neurons
P1/P2 * 100
P1/P3 Type I - Week 3
# of Neurons
P1/P3 * 100

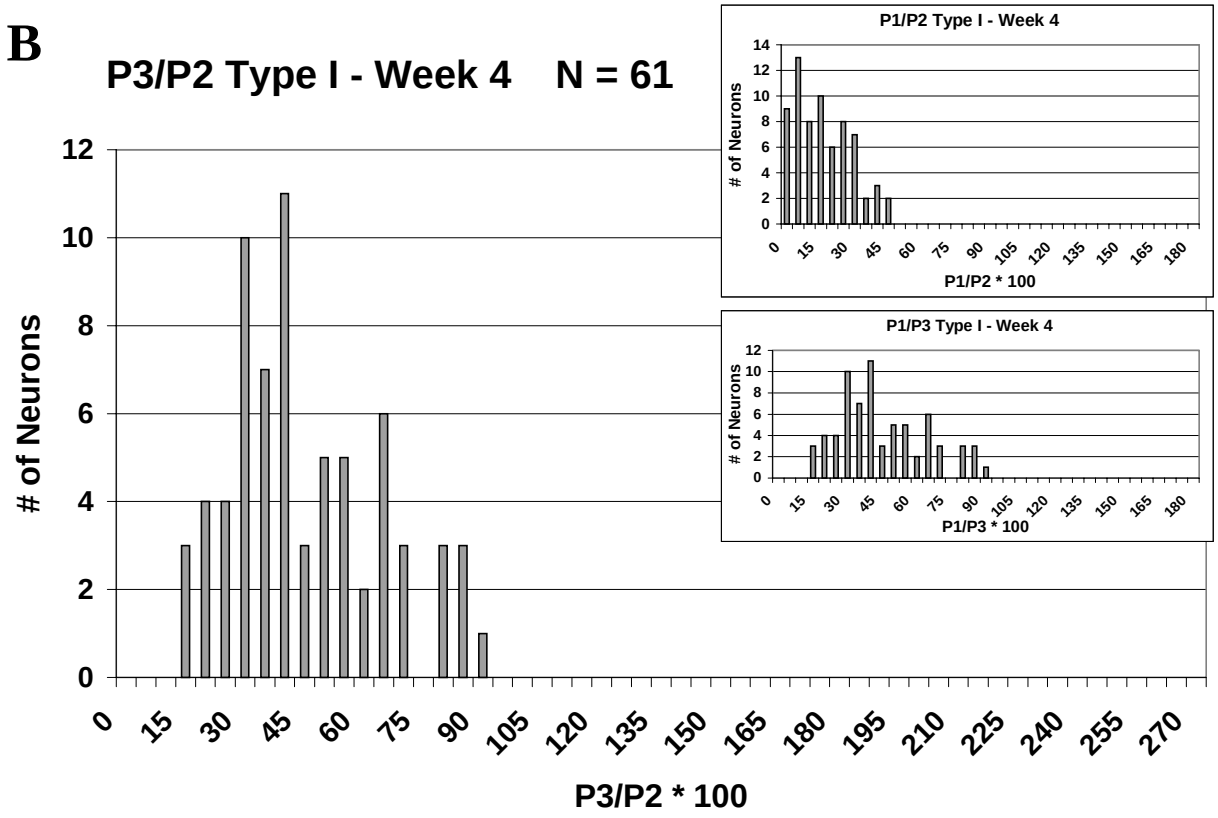
B
P3/P2 Type I - Week 4 N = 61
# of Neurons
P3/P2 * 100
P1/P2 Type I - Week 4
# of Neurons
P1/P2 * 100
P1/P3 Type I - Week 4
# of Neurons
P1/P3 * 100

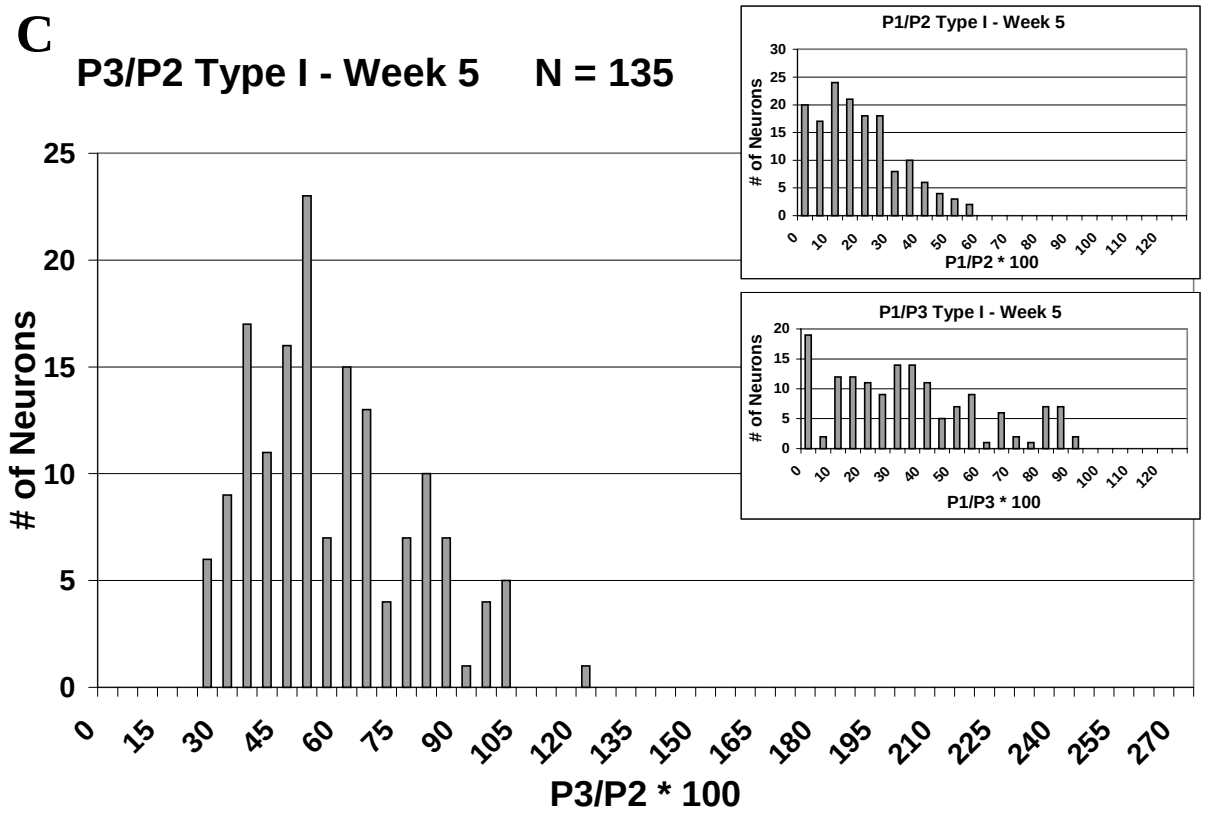
C
P3/P2 Type I - Week 5 N = 135
# of Neurons
P3/P2 * 100
P1/P2 Type I - Week 5
# of Neurons
P1/P2 * 100
P1/P3 Type I - Week 5
# of Neurons
P1/P3 * 100

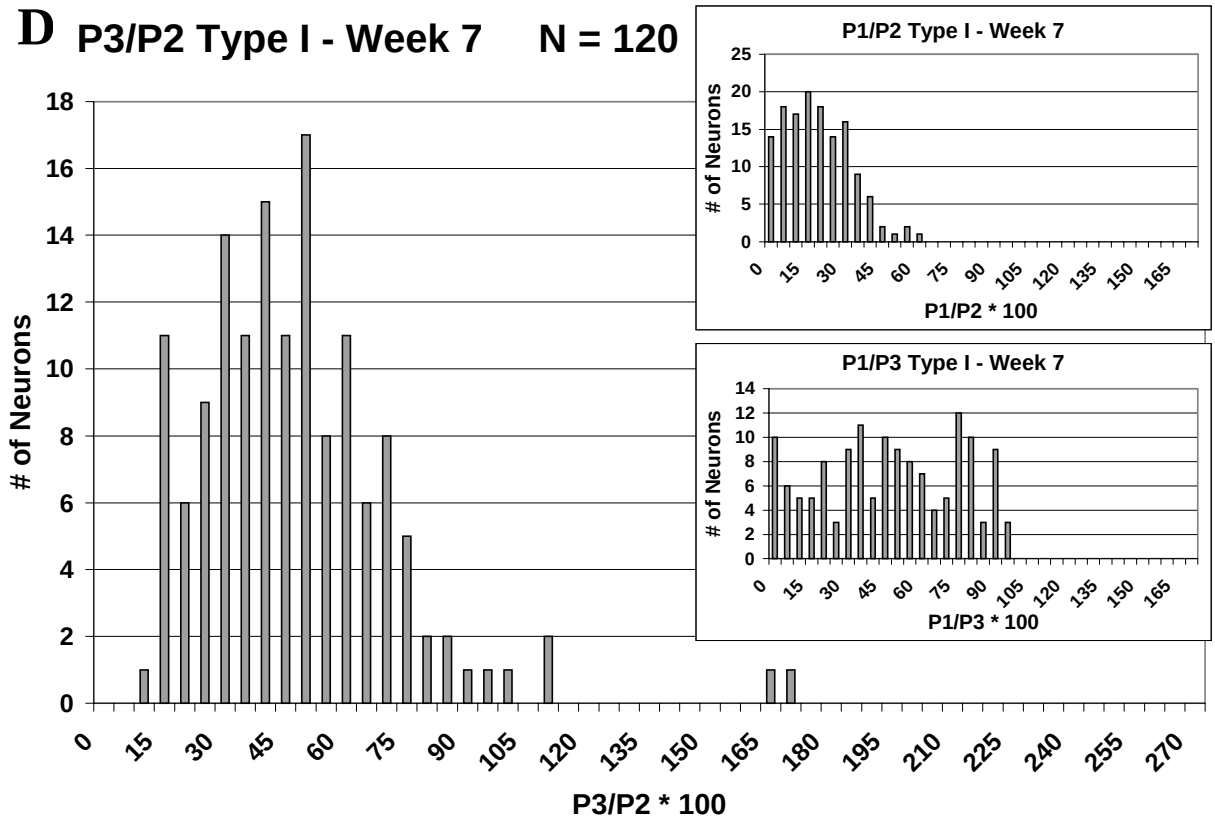
D
P3/P2 Type I - Week 7 N = 120
# of Neurons
P3/P2 * 100
P1/P2 Type I - Week 7
# of Neurons
P1/P2 * 100
P1/P3 Type I - Week 7
# of Neurons
P1/P3 * 100

(Pages 37 – 38) Figure 16: NORMALIZED PEAK AMPLITUDE HISTIGRAMS. The distributions of peak 3 to peak 2 ratios are not significantly different for weeks 3, 4, 5, and 7 according to the Kruskal-Wallis test ($p > 0.05$). This could imply that developmental changes occur in Na^+ channel concentration must be mirrored by K^+ channel changes. Inserts show the distribution of ratios for P1 / P2 and P1 / P3.

4.6 Developmental Changes in Type II Signals

The most noticeable change in type II passive signals was the increase in the number of signals from an average of 7 per culture to 17 per culture from weeks 3 through 7. There was no trend in the amplitudes of the type II signals with age, which ranged from 59.9 to 77.0 μV (Figure 18, section 5.4). A characteristic peak 1 to peak 2 distribution was generated using all the type II signals from all ages, and showed a peak at peak 1 being just over 40 % of peak 2 (Figure 18). However, in comparing peak 3 to peak 1 over all the ages showed a tendency for three groups to emerge as three distinct types of type II signals (Figure 19). It should also be noted that in some cases, certain type II signals would spontaneously change into type I signals throughout the course of an experiment. This event occurred exclusively with those signals which had the higher peak 3 to peak 1 ratios (> 60).

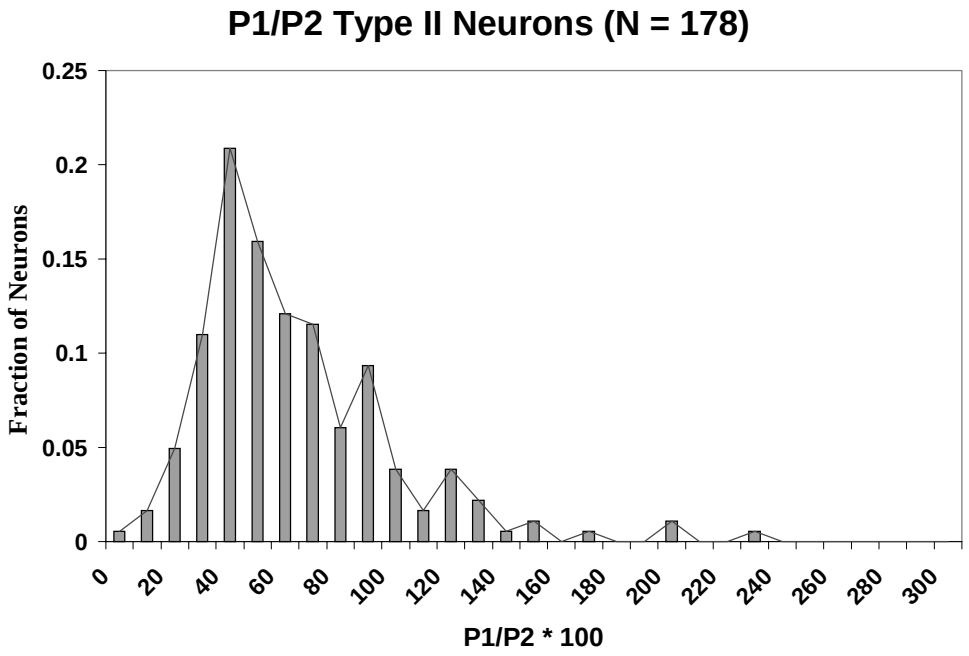

Figure 17: NORMALIZE TYPE II AMPLITUDE HISTIGRAM. The distribution curve for the ratio of peak 1 to peak 2 in type II signals showing a maximum at P1 / P2 * 100 between 40 and 50. This curve was generated using all of the data from every age in the development study.

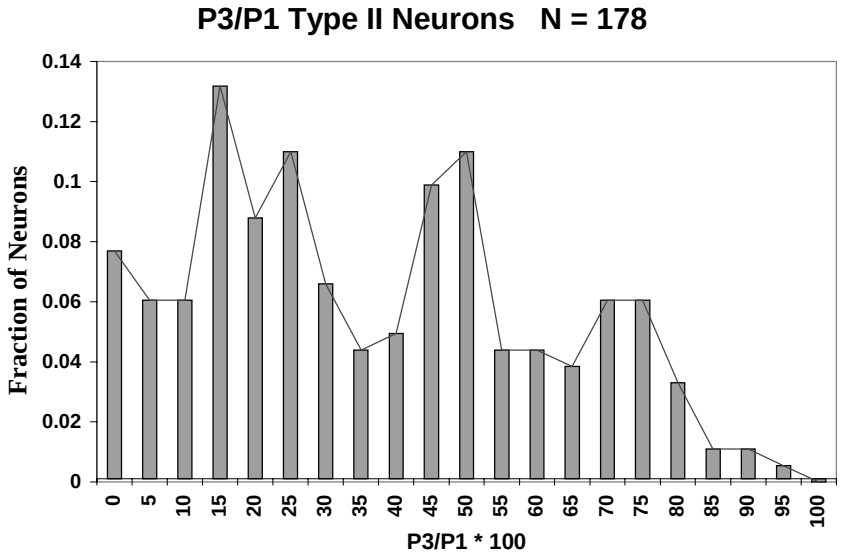

Figure 18: PEAK 3 TO PEAK 1 RATIO FOR TYPE II. A distribution of peak 3 to peak 1 rations displaying three distinct grouping of type II signals based on the size of peak 3.

CHAPTER 5

DISCUSSION

5.1 Temperature Studies

The temperature studies demonstrate how closely the array recording environment mimics the *in vivo* data. It is well known that reductions in temperature slows the opening of ion channels and the rate of diffusion for ions through the channels, thereby widening and reducing the amplitude of electrical signals [Bostock et al., 1981]. The interesting phenomenon here is that approximately 30 percent of neurons actually increased in amplitude. All neurons increased in width. The explanation of this remains to be demonstrated but it may have to do with the fact that conductances of ion channels were not reduced but the kinetics for closing was delayed thereby allowing more current to flow during the action potential.

5.2 K^+ Channel Blocker Studies

A number of different types of cells, which can be found in spinal cord tissue, are reported to have very different responses to TEA. Although, not a large amount of specific literature exists on interneurons, ventrolateral medulla interneurons display an increase in width due to TEA [Ballanyi et al., 1999]. Motoneurons are reported to increase substantially in width to TEA but not as much to 4AP [Gao and Ziskand, 1998]. TEA does not seem to decrease amplitudes for motoneurons [Booth et al., 1997]. No report was found observing an increase in signal peak to peak amplitudes for spinal cord neurons in response to TEA. In our results is that 15 % of our recorded signals in spinal cord did increase peak 3 amplitude in response to TEA.

There are recordings of pyramidal interneurons in frontal cortex tissue increasing in amplitude in response to TEA [Chen et al., 1996].

4-aminopyridine is known to lengthen the action potential for many different cell types throughout the CNS. For spinal cord, there are several studies reported for 4AP due to its potential use for treating multiple sclerosis. In demylenated dorsal roots at 5 mM 4AP, amplitudes increased and widen dramatically using intracellular recording [Sherratt et al., 1980]. Also, demylenated ventral root fiber and C-fiber signals widened but the amplitude change was minimal [Bostock et al., 1981]. For frontal cortex tissue, there is little literature concerning the effects of 4AP. There is a prominent report concerning Layer V of motor cortex where the pyramidal and interneurons are reported to increase in width but only increase in amplitude for narrow signals [Chen et al., 1996]. In our study, more Type I signals (56.4 %) in each culture responded to 4AP by widening their negative signals than widened in response to TEA (20.4 %). The same held true for the peak 3 of Type I (60.1 % for 4AP and 53.9 % for TEA). Also, more Type I neurons in each culture increased their amplitude of peak 2 and peak 3 to 4AP (20.8 % and 17.4 %, respectively) than to TEA (17.4 % and 15.2 %). These differences reflect that more Type I signals were unresponsive to TEA than to 4AP – 44.1 % versus 34.7 %. Of course, since this comparison is between different tissue types and this observation reflects a difference in drug mechanisms as well as difference in populations of cell types.

5.3 Na^+ Channel Modulator Studies

As mentioned before, attempts to show modulation of Na^+ channels were largely unsuccessful. This is due to the complex dynamics of Na^+ channel populations that regulate

excitability. TTX blocks Na^+ channels and apparently lowers the concentration of Na^+ channels so that all activity ceases. It is possible that a small ~ 5 – 10 % fluctuation in Na channel concentration can move the activation curve well beyond the range of the largest integrated input signals. In studies using spontaneously active cultures, measurements cannot be made when activity stops. However, 58 % of signals responded to monensin but with relatively small changes in their amplitudes. Literature suggests that there must be a receptor for monensin to be able to enter the cell, therefore making measurements even more difficult. Also, the effect was on the peak-to-peak amplitude showing that K^+ currents are definitely linked to Na^+ currents, as would be expected.

5.4 Developmental Studies

The main result of the developmental studies is that both the number and amplitude of active, type I, units increase with age. This reflects the published observations that there are key pre- and post-natal developmental stages in animals where reorganization occurs in the ion channels allowing for a lower activation threshold and easier action potential initiation [Gao and Ziskand, 1998]. The occurrence of a similar phenomenon in culture suggests an predetermined developmental sequence established before the point of dissection. However, the increase in amplitudes can be attributed to either changes in cell-electrode coupling or ion channel expression (Figure 20).

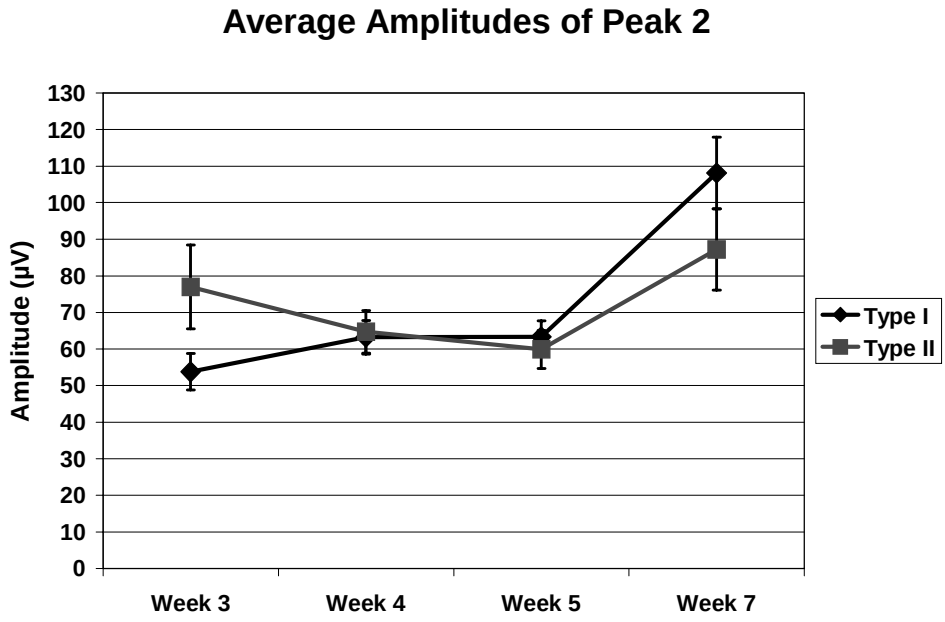

Figure 19: TEMPORAL CHANGES IN WAVESHAPE AMPLITUDES. Type I signals show a consistent developmental increase in amplitude of peak 2 while type II decrease and then return to the amplitude level in week 7 as in week 3. Error bars reflect standard deviations.

Secondly, the consistent distribution for the ratio of peak 3 to peak 2 points towards parallel development of both Na^+ and K^+ channels. The cause of the maxima in the distribution of peak 3 to peak 1 for type II signals is unexplained (Figure 19). It is suspected that these are examples of wholly passive and partially active signal transduction, especially since those signals with larger peak 3's had the ability to spontaneously switch to type I signals. This is not surprising since dendrites often have high densities of voltage-gated ion channels even though the concentration is not high enough for excitability [Safronov, 1999].

Finally, there was noted a significant difference in the number of passive signals between spinal cord (33 %) and frontal cortex (18 %). This is in excellent agreement with published studies suggesting that spinal cord dendrites and somas are unable to support back-propagating

action potentials, which are known to be quite common in cortical pyramidal cells [Safronov, 1999; Stuart et al., 1997]. Therefore, the possibility of active dendritic signals in cortical tissue would reduce the probability of passive dendritic signals being observed.

5.5 Conclusions

The conclusions of this study are that ion channel contributions to signal shape can be demonstrated using multielectrode arrays. The data presented identify type I signals as active action potential propagation; and, more specifically, peak 3 of type I as the K^+ current. The visualization of these effects along with simultaneous firing pattern recordings offers an interesting new tool for membrane plasticity research. Finally, developmental research may allow the study of the extent to which intrinsic neuron properties are preserved in culture.

APPENDIX

CODE USED FOR VISUAL BASIC MACROS IN MS EXCEL™

```
Sub Macro1()
'
' Macro1 Macro
' Macro recorded 1/24/2003 by Lab
'

'
    ActiveChart.Axes(xlValue).Select
    With ActiveChart.Axes(xlValue)
        .MinimumScaleIsAuto = True
        .MaximumScaleIsAuto = True
        .MinorUnitIsAuto = True
        .MajorUnit = 10
        .Crosses = xlAutomatic
        .ReversePlotOrder = False
        .ScaleType = xlLinear
        .DisplayUnit = xlNone
    End With
End Sub
Sub Macro2()
'
' Macro2 Macro
' Macro recorded 1/24/2003 by Lab
```

```
'


'
    ActiveChart.Axes(xlValue).Select
    With ActiveChart.Axes(xlValue)
        .MinimumScaleIsAuto = True
        .MaximumScaleIsAuto = True
        .MinorUnitIsAuto = True
        .MajorUnit = 5
        .Crosses = xlAutomatic
        .ReversePlotOrder = False
        .ScaleType = xlLinear
        .DisplayUnit = xlNone
    End With
End Sub


Sub Macro3()
'
' Macro3 Macro
' Macro recorded 1/27/2003 by Lab
'


'
```

```
    ActiveChart.ChartArea.Select
    ActiveChart.ChartArea.Copy
End Sub

Sub Macro4()
'
' Macro4 Macro
' Macro recorded 2/28/2003 by Lab
'

'

  For i = 1 To Worksheets.Count
      Worksheets(i).Activate


    Range("bh5:bj40").Select
    Selection.Copy
    Range("bn5").Select
    ActiveSheet.Paste

    Range(Selection, Selection.End(xlToRight)).Select
    Range("bh130:bj165").Select
```

```
Selection.Copy


Range("Bq5").Select
ActiveSheet.Paste
Columns("Bn:Bn").Select
Application.CutCopyMode = False
Columns("bo:bo").Select
Selection.Insert Shift:=xlToRight
Columns("Bq:Bq").Select
Selection.Insert Shift:=xlToRight
Columns("Bs:Bs").Select
Selection.Cut Destination:=Columns("bo:bo")
Columns("Bt:Bt").Select
Selection.Cut Destination:=Columns("Bq:Bq")
Columns("Bu:Bu").Select
Selection.Cut Destination:=Columns("Bs:Bs")
Range("bn4").Select
ActiveCell.FormulaR1C1 = "P1 B4"
Range("bo4").Select
ActiveCell.FormulaR1C1 = "P1 After"
Range("bp4").Select
ActiveCell.FormulaR1C1 = "P2 B4"
Range("Bq4").Select
```

```
    ActiveCell.FormulaR1C1 = "P2 After"
    Range("Br4").Select
    ActiveCell.FormulaR1C1 = "P3 B4"
    Range("Bt4").Select
    ActiveCell.FormulaR1C1 = "P3 After"
    Range("bn5:bo5").Select
    Range(Selection, Selection.End(xlDown)).Select

    Application.Run "ATPVBAEN.XLA!Pttestv", ActiveSheet.Range("$bn$5:$bn$40"), _
       ActiveSheet.Range("$bo$5:$bo$40"), ActiveSheet.Range("$Bu$4:$Bz$21"), False _
       , 0.05
     Application.Run "ATPVBAEN.XLA!Pttestv", ActiveSheet.Range("$bp$5:$bp$40"), _
       ActiveSheet.Range("$Bq$5:$Bq$40"), ActiveSheet.Range("$Bu$19:$Bz$34"), False _
       , 0.05
     Application.Run "ATPVBAEN.XLA!Pttestv", ActiveSheet.Range("$Br$5:$Br$40"), _
       ActiveSheet.Range("$Bs$5:$Bs$40"), ActiveSheet.Range("$Bu$34:$Bz$51"), False _
       , 0.05
    Next i


End Sub
```

```
Sub Macro5()
'
' Macro5 Macro
' Macro recorded 2/28/2003 by Lab
'

'


 For i = 1 To Worksheets.Count
       Worksheets(i).Activate


    Range("By7").Select
    ActiveCell.FormulaR1C1 = "=(RC[-2]-RC[-3]) / RC[-3]"
    Range("By8").Select
    ActiveCell.FormulaR1C1 = "=RC[-2]"
    Range("By8").Select
    ActiveCell.FormulaR1C1 = "=(RC[-2]-RC[-3])/RC[-3]"
    Range("By7").Select


    Range("By9").Select
    ActiveCell.FormulaR1C1 = "=ABS(R[3]C[-3]) - R[7]C[-3]"
    Range("By7:By9").Select
    Selection.Copy
```

```
    Range("By22").Select
    ActiveSheet.Paste
    Range("By37").Select
    ActiveSheet.Paste
    Next i
End Sub
Sub Macro6()
'
' Macro6 Macro
' Macro recorded 2/28/2003 by Lab
'

'

Dim n As Integer
n = 0

  For i = 1 To Worksheets.Count

    Worksheets(i).Select
    Range("By7:By9").Select
    Selection.Copy
    Sheets("Sheet1").Select
```

```
    Cells(5, i + 1).Select
    ActiveSheet.Paste Link:=True
    Cells(8, i + 1).Select
    Worksheets(i).Select
    Range("By22:By24").Select
    Application.CutCopyMode = False
    Selection.Copy
    Sheets("Sheet1").Select
    ActiveSheet.Paste Link:=True
    Cells(11, i + 1).Select
    Worksheets(i).Select
    Range("By37:By39").Select
    Application.CutCopyMode = False
    Selection.Copy
    Sheets("Sheet1").Select
    ActiveSheet.Paste Link:=True
    Cells(4, i + 1).Select
    ActiveCell.FormulaR1C1 = "Unit" & n
    n = n + 1

    Next i

End Sub
```

```
Sub Macro7()
'
' Macro7 Macro
' Macro recorded 5/12/2003 by Lab
'

'

For i = 1 To Worksheets.Count
      Worksheets(i).Activate

   Columns("BN:BY").Select
   Selection.ClearContents

   Next i

End Sub
Sub Macro8()
'
' Macro8 Macro
' Macro recorded 5/12/2003 by Lab
'
```

```
Dim n As Integer
n = 0

  For i = 1 To Worksheets.Count

    Worksheets(i).Select

    If Range("bn6").Cells(1) > Range("br6").Cells(1) Then
       Range("By7:By9").Select
       Selection.Copy
       Sheets("Sheet1").Select
       Cells(18, i + 1).Select
       ActiveSheet.Paste Link:=True
       Cells(21, i + 1).Select
       Worksheets(i).Select
       Range("By22:By24").Select
       Application.CutCopyMode = False
       Selection.Copy
       Sheets("Sheet1").Select
       ActiveSheet.Paste Link:=True
       Cells(24, i + 1).Select
       Worksheets(i).Select
```

```
    Range("By37:By39").Select
    Application.CutCopyMode = False
    Selection.Copy
    Sheets("Sheet1").Select
    ActiveSheet.Paste Link:=True
    Cells(17, i + 1).Select
    ActiveCell.FormulaR1C1 = "Unit" & n
    n = n + 1
    End If

If Range("bn6").Cells(1) < Range("br6").Cells(1) Then
    Range("By7:By9").Select
    Selection.Copy
    Sheets("Sheet1").Select
    Cells(30, i + 1).Select
    ActiveSheet.Paste Link:=True
    Cells(33, i + 1).Select
    Worksheets(i).Select
    Range("By22:By24").Select
    Application.CutCopyMode = False
    Selection.Copy
    Sheets("Sheet1").Select
    ActiveSheet.Paste Link:=True
```

```
        Cells(36, i + 1).Select
        Worksheets(i).Select
        Range("By37:By39").Select
        Application.CutCopyMode = False
        Selection.Copy
        Sheets("Sheet1").Select
        ActiveSheet.Paste Link:=True
        Cells(29, i + 1).Select
        ActiveCell.FormulaR1C1 = "Unit" & n
        n = n + 1
        End If

    Next i

End Sub
```

REFERENCES

Ballanyi, K, Onimaru, H, & Homma, I (1999) Respiratory network function in the isolated brainstem-spinal cord of newborn rats. *Progress in Neurobio* 59, 583-634.

Baro, DJ, Ayali, A, French, L, Scholz, NL, Labenia, J, Lanning, CC, Graubard, K, Harris-Warrick, RM (2000), Molecular underpinnings of motor pattern generation: differential targeting of shal and shaker in the pyloric motor system, *J of Neurosci* 20(17), 6619-6630.

Booth, V., Rinzel, J., & Kiehn, O., (1997), Compartmental model of vertebrate motoneurons, *J Neurophysiol* 78, 3371-3385.

Bostock, H., Sears, T. A., & Sherratt, R. M. (1981). The effects of 4-aminopyridine and tetraethylammonium ions on normal and demylenated mammalian nerve fibers. *J Physiol* 313, 301-315.

Bowe, C.M., Kocsis, J.D., Waxman, S.G. (1985) Differences between mammalian ventral and dorsal spinal roots in response to blockade of potassium channels during maturation. *Proc. R. Soc. Lond. B* 224, 355-366.

Chen, W., Zhang, J.-J., Hu, G.-Y.,Wu, C.-P. (1996) Different mechanisms underlying the repolarization of narrow and wide action potentials in pyramidal cells and interneurons of cat motor cortex. *Neuroscience* 73 (1), 57-68.

Crain, S. M. (1998). Development of specific synaptic network functions in organotypic central nervous system (CNS) cultures: implications for transplantation of CNS neural cells *in vivo*. *Methods Enzymology* 16, 228-238.

Dhingra, N.K., Reddy, R., Govindaiah, Hemavathy, U., Raju, T.R., Ramamohan, Y. (2001). Synaptic development in semi-dissociated cultures of rat retina. *Int. J. Devl Neuroscience* 19, 533-540.

Eccles, JC (1957). *The physiology of nerve cells*. Johns Hopkins Press, Baltimore.

Eccles, JC, Libet, B, Young RR (1958) The behavior of chromatolysed motoneurons studied by intracellular recording, *J. Physiol*, 143, 11-40.

Freygang, W.H., & Frank, K. (1959) Extracellular potentials from single spinal motoneurons. *J Gen Physiol* 42: 749-760.

Gao, B.-X., & Ziskind-Conhaim, L. (1998) Development of ionic currents underlying changes in action potential waveforms in rat spinal motoneurons. *J Neurophysio* 86(1), 492-502.

Gopal, KV, & Gross, GW (1996). Auditory cortical neurons in vitro: cell culture and multichannel extracellular recording. *Acta Otolaryngol* 116:690-696.

Gopal, KV, & Gross GW (1996). Auditory cortical neurons in vitro: initial pharmacological studies. *Acta Otolaryngol* 116:697-704.

Gramowski, A., Schiffmann, D., & Gross, G. W. (2000). Quantification of acute neurotoxic effects of trimethyltin using neuronal networks cultured on microelectrode arrays. *Neurotoxicology 2*1, 331-342.

Gray, C. M., Maldonado, P. E., Wilson, M., McNaughton, B. (1995). Tetrodes markedly improve the reliability and yield of multiple single-unit isolations from multi-unit recordings in cat striate cortex. *J Neuro Methods* 63, 43-54.

Gross, G. W., Kowalski, J. W. (1991). Experimental and theoretical analysis of random network dynamics, in: P. Antognett, V. Multinovic (Eds.), *Neural Networks,*

Concepts, Application and Implementations, Vol. 4, Prentice-Hall, New Jersey, 277-317.

Gross, G. W., Rhoades, B., & Jordan R. (1992). Neuronal networks for biochemical sensing. *Sensors and Actuators B* 6, 1-8.

Gross, G. W., Rhoades, B. K., Azzazy, H. M. E., & Wu, M. (1995). The use of neuronal networks on multielectrode arrays as biosensors. *Biosensors & Bioelectronics* 10, 553-567.

Gross, G. W., Norton, S., Gopal, K., Schiffmann, D., & Gramowski, A. (1997). Neuronal networks in vitro: applications to neurotoxicology, drug development and biosensors. *Cellular Engineering* 2, 138-147.

Harris-Warrick, RM (2002). Voltage-sensative ion channels in rhythmic motor systems. *Current Opinions in Neurobiol* 12:646-651.

Henze, D. A., Borhegyi, Z., Csicsveri, J., Mamiya, A., Harris, K. D., Buzsaki, G. (2000). Intracellular features predicted by extracellular recordings in the hippocampus in vivo. *J. Neurophysiol* 84:390-400.

Hille, B. (1992). *Ionic channels of excitable membranes*, 2nd Ed. Sinauer Associates Inc., Sunderland, Mass.

Holt, G. R. (1998). A critical reexamination of some assumptions and implications of cable theory in neurobiology. Ph. D. Thesis, California Institute of Technology, Computational and Neural Systems Program.

Hodgkin, A. L., & Huxley, A. F. (1952) A quantitative description of membrane current and its application to conduction and excitation in nerve. *J. Physiol (Lond)* 117, 500-544.

Humphrey, D. R. (1968) Re-analysis of the antidromic cortical response. II. On the contributions of cell discharge and PSPs to the evoked potentials. *Electroenceph. Clin. Neurophysio.* 25, 421-442.

Institute of Laboratory Animal Resources, Commission on Life Sciences, National Research Council. (1996). *Guide for the Care and Use of Laboratory Animal*s. Washington, DC: National Academy Press.

Kandel, E.R., Schwartz, J.H., Jessell, T.M. (1991) *Principles of Neural Science*, 4th Ed., McGraw-Hill, New York.

Kaneko, S, Okada, M, Iwasa, H, Yamakawa, K, Hirose, S (2002). Genetics of epilepsy: currents status and perspectives. *Neurosci Research* 44, 11-30.

Katz, MJ (1985). How straight do axons grow? *J Neurosci* 5, 589-595.

Keefer, E. W., Gramowski, A., & Gross, G. W. (2001a). NMDA receptor-dependent periodic oscillations in cultured spinal cord networks. *J Neurophysiol 8*6, 3030-3042.

Keefer, E. W., Gramowski, A., Stenger, D. A., Pancrazio, J. J., & Gross, G. W. (2001b). Characterization of adscute neurotoxic effects of trimethy-lolpropane phosphate via neuronal network biosensors. *Biosens Bioelec-tron 1*6, 513-525.

Keefer, E. W., Norton, S. J., Boyle, N. A. J., Talesa, V., & Gross, G. W. (2001c). Acute toxicity screening of novel AChE inhibitors using neuronal networks on microelectrode arrays. *Neurotoxicology 2*2, 3-12.

Kobayashi, J., Ohta, M., & Terada, Y., (1998) Differentail contribution of Na-K pump and K conductance to the post-tetanic hyperpolarization of the subtypes of tetrodotoxin-resistant C-fibers in the isolated bullfrog sciatic nerve. *Neurosci*

Letters 242, 57-60.

Koch, C, & Poggio, T (1987) Biophysics of computation: neurons, synapses, and membranes. In: Edelman, GM, Gall, WE, & Cowan, WM (Eds), *Synaptic Function*. John Wiley & Sons, New York, 637-697.

Kocsis, J.D., Waxman, S.G., Hildebrand, C., Ruiz, J.A. (1982). Regenerating mammalian nerve fibres: changes in action potential waveform and firing characteristics following blockage of potassium conductance. *Proc. R. Soc. Lon. B* 217, 77-87.

Kuno, M., Llinas, R (1970) Enhancement of synaptic transmission by dendritic potentials in chromatolysed motoneurons of the cat. *J Physiol Lond* 210, 807-821.

Lasek, RJ (1988), Studying the intrinsic determinant of neuronal form and function, In: Lasek, RJ, & Black MM (eds), *Intrinsic determinants of neuronal form and function*, Neurology and Neurobiology, Vol. 37, Alan R. Liss, Inc., New York, 1-60.

Levitan, IB, & Kaczmarek, LK (1991) *The Neuron: Cell and Molecular Biology*. Oxford University Press, New York.

Llinas, R., & Nicholson, C. (1971) Electrophysiological properties of dendrites and somata in alligator Purkinje cells. *J Neurophysiol* 34 (4), 532-551.

Meunier, C., & Segev, I. (2002). Review: Playing the Devil's advocate: is the Hodgkin-Huxley model useful? *TRENDS in Neuro* 25, 558-563.

Morefield, S. I., Keefer, E. W., Chapman, K. D., &Gross, G. W. (2000). Drug evaluations using neuronal networks cultured on microelectrode arrays. *Biosens Bioelectron* 15, 383-396.

Nashmi, R., & Fehlings, M. G. (2001). Mechanisms of axonal dysfunction after spinal cord injury: with an emphasis on the role of voltage-gated potassium channels. *Brain Research Reviews* 38, 165-191.

Novakovic, SD, Eglen, RM, Hunter, JC (2001). Regulation of Na channel distributions in the nervous system. *TRENDs in Neuro* 24 (8), 473-477.

O'Shaughnessy, T. J., Zim, B., Ma, W., Shaffer, K. M., Stenger, D. A., Zamani, K., Gross, G. W., Pancrazio, J. J. (2003) Acute neuropharmacologic action of chloroquine on cortical neurons in vitro. *Brain Research* 959, 280-286.

Pancrazio, J.J., Keefer, E. W., Ma, W., Stenger, D. A., Gross, G. W. (2001). Neurophysiologic effects of chemical agent hydrolysis products on cortical neurons in vitro. *NueroToxicology* 22, 393-400.

Quasthoff, S., Grosskreutz, J., Schroder, J. M., Schneider, U., & Grafe, P. (1995) Calcium potentials and tetrodotoxin-resistant sodium potentials in unmylenated C fibres of biopsied human sural nerve. *Neuroscience* 69, 3, 955-965.

Rall, W. (1962). Electrophysiology of a dendritic neuron model. *Biophys. J.* 2:145-167.

Rampon, C., Luppi, P.H., Fort, P., Peyron, C., & Jouvet, M. (1996). Distribution of glycine-immunoreactive cell bodies and fibers in the rat brain. *Neuroscience* 75 (3), 737-755.

Ransom, B. R., Neale, E., Henkart, M., Bullock, P. N., & Nelson, P. G. (1977). Mouse spinal cord in cell culture. I. Morphology and intrinsic neuronal electrophysiologic properties. *J Neurophysiol* 40, 1132–1150.

Rashid, AJ, Morales, E, Turner, RW, Dunn, RJ (2001). The contribution of dendritic Kv3 K^+ channels to burst threshold in a sensory neuron. *J of Neuro* 21(1), 125-135.

Reganathan, M., Gelderblom, M., Black, J.A., Waxman, S.G. (2003). Expression of Na_v 1.8 sodium channels perturbs the firing patterns of cerebullar purkinje cells. *Brain Research* 959, 235-242.

Safronov, BV. (1999) Spatial distribution of Na^+ and K^+ channels in spinal dorsal horn neurons: role of the soma, axon and dendrites in spike generation. *Prog Neurobiol* 59(3):217-241.

Selinger, JV, Pancrazio, JJ, Gross, GW. (2003) Measuring synchronization in neuronal networks for biosensor applications. *Biosensors and Bioelectronics* 1126:1-9.

Sherratt, R.M., Bostock, H., Sears, T. A. (1980) Effects of 4-aminopyridine on normal and demylenated mammalian nerve fibres. *Nature* 283, 570-572.

Stuart, G., Spruston, N., Sakmann, B., Hausser, M. (1997) Action potential initiation and backpropagation in neurons of the mammalian CNS. *Trends in Neuro* 20, 125-131.

Traub, RD, Jeffreys, JGR, & Whittington, MA (1999) *Fast oscillations in cortical circuits*. The MIT Press, Cambridge, Mass.

Verbny, Y., Zhang, CL, Chiu, SY (2002) Coupling of calcium homeostasis to axonal sodiums in axons of mouse optic nerve. *J Neurophysiol* 88(2):802-816.

Waxman, S.G., Ritchie, J.M. (1985) Organization of ion channels in the mylenated nerve fiber. *Science*, New Series, 228 (4707), 1502-1507.

Waxman, S.G. (1999). The molecular pathophysiology of pain: abnormal expression of sodium channel genes and its contributions to hyperexcitability of primary sensory neurons. *Pain* 82: (Supp. 1) S133-S140.

Waxman, S.G., Dib-Hijj, S., Cummins, T.R., Black, J.A. (2000). Sodium channels and their genes: dynamics expression in the normal nervous system, dysregulation in disease states. *Brain Research* 886, 5-14.

Waxman, S.G., (1995) SL-2: Ion channels and nerve conduction. *Electroenceph. and Clinical Neurophys./ Electromyo. and Motor Control* 97 (4): S1.

Xia, Y., Gopal, K.V., Gross, G.W. (2003) Differential acute effects of fluoxetine on frontal and auditory cortex networks in vitro. *Brain Research* 973, 151-160.

Xia, Y., Gross, G.W. (2003) Histiotypic responses of neuronal networks *in vitro* to ethanol. *Alchohol* 30, 1-8.

Yu, FH, Catterall, WA (2003). Overview of the voltage-gated sodium channel family. *Genome Biol* 4 (3).